

Article

# Cosmeceutical Potentials of *Equisetum debile* Roxb. ex Vaucher Extracts

Phanit Thammarat<sup>1,2</sup>, Jutamas Jiaranaikulwanitch<sup>1,2,\*</sup> , Rungsinee Phongpradist<sup>1,2</sup>, Araya Raiwa<sup>1</sup>, Hataichanok Pandith<sup>3,4</sup>, Kasirawat Sawangrat<sup>1,2</sup> and Sasithorn Sirilun<sup>1,5,\*</sup> 

<sup>1</sup> Department of Pharmaceutical Sciences, Faculty of Pharmacy, Chiang Mai University, Chiang Mai 50200, Thailand

<sup>2</sup> Center of Excellence for Innovation in Analytical Science and Technology for Biodiversity-Based Economic and Society (I-ANALY-S-T\_B.BES-CMU), Chiang Mai University, Chiang Mai 50200, Thailand

<sup>3</sup> Department of Biology, Faculty of Sciences, Chiang Mai University, Chiang Mai 50200, Thailand

<sup>4</sup> Research Center in Bioresources for Agriculture, Industry and Medicine, Faculty of Science, Chiang Mai University, Chiang Mai 50200, Thailand

<sup>5</sup> Innovation Center for Holistic Health, Nutraceuticals, and Cosmeceuticals, Faculty of Pharmacy, Chiang Mai University, Chiang Mai 50200, Thailand

\* Correspondence: jutamas.jia@cmu.ac.th (J.J.); sasithorn.s@cmu.ac.th (S.S.); Tel.: +66-5394-4382 (J.J.)

**Abstract:** Trends in skin and hair treatments focus on natural products due to undesired effects of chemically synthetic ingredients. This study aims to investigate the cosmeceutical effects of *Equisetum debile* (horsetail) extracts relating to anti-hyperpigmentation via tyrosinase, anti-wrinkle formation via matrix metalloproteinases (MMPs), and anti-androgenic alopecia via 5 $\alpha$ -reductase. Ethanolic extracts were sequentially partitioned into semi-purified fractions hexane, dichloromethane, ethyl acetate, methanol, and methanol insoluble residue. The ethyl acetate fraction possessed the highest total phenolic content ( $39.24 \pm 0.72$  mg gallic acid/g), the strongest anti-tyrosinase activities ( $583.33 \pm 23.59$  mg kojic acid/g), and potent collagenase inhibitions (IC<sub>50</sub> MMP-1 and MMP-2 of  $0.82 \pm 0.09$  and  $0.94 \pm 0.11$  mg/mL, respectively). All extracts showed considerable inhibitions of 5 $\alpha$ -reductase ranging from  $44.59 \pm 0.40$  to  $83.07 \pm 3.46\%$  with the strongest activity from the dichloromethane fraction ( $1.48 \pm 0.06$  mg finasteride/g). In conclusion, *E. debile* extracts exhibit cosmeceutical potentials. This study suggests that the *E. debile* ethyl acetate fraction could be used as a promising ingredient to organically treat hyperpigmentation and delay the skin aging process. In addition, compared to the current recommended intake of finasteride (1 mg/day) for androgenic alopecia, the dichloromethane fraction is proposed as an alternative source to naturally remediate hair loss.

**Keywords:** natural product; *Equisetum*; horsetail; tyrosinase; collagenase; 5 $\alpha$ -reductase; hair; skin; whitening; wrinkle



**Citation:** Thammarat, P.; Jiaranaikulwanitch, J.; Phongpradist, R.; Raiwa, A.; Pandith, H.; Sawangrat, K.; Sirilun, S. Cosmeceutical Potentials of *Equisetum debile* Roxb. ex Vaucher Extracts. *Appl. Sci.* **2023**, *13*, 1336. <https://doi.org/10.3390/app13031336>

Academic Editors: António José Madeira Nogueira and Andrea Luísa Fernandes Afonso

Received: 15 December 2022

Revised: 15 January 2023

Accepted: 17 January 2023

Published: 19 January 2023



**Copyright:** © 2023 by the authors. Licensee MDPI, Basel, Switzerland. This article is an open access article distributed under the terms and conditions of the Creative Commons Attribution (CC BY) license (<https://creativecommons.org/licenses/by/4.0/>).

## 1. Introduction

Skin hyperpigmentation, wrinkles, and hair loss are not life-threatening conditions but are serious concerns leading to higher risks of social pressure, low self-esteem, and depression [1,2]. Tyrosinase, collagenases, and 5 $\alpha$ -reductase are the most studied enzymes for potential remedies of skin and hair problems. The reactive oxygen species (ROS) induced by ultraviolet (UV) radiation can cause skin hyperpigmentation disorders and photoaging by oxidative damage of skin lipids, proteins, and DNA and setting off enzymatic cascades relating to tyrosinase and collagenases [3]. UV radiation is also the most significant risk factor for nonmelanoma and melanoma skin cancers [4–7].

Tyrosinase, a rate-limiting enzyme in melanogenesis, catalyzes a series of oxidations converting L-tyrosine to 3,4-dihydroxyphenyl-L-alanine (L-DOPA) and dopaquinone. The polymerization of several dopaquinones then gives rise to melanin, causing skin to darken [6,8]. Melanin normally protects skin from UV radiation via shielding effects. It serves as a physical barrier scattering UV and an absorbent filter reducing UV penetration through the epidermis [9]. However, when tyrosinase is overactivated by UV-induced ROS, it causes unpleasant skin hyperpigmentation disorders such as pigmented acne scars, senile lentigo, melasma, and freckles [10,11].

Collagenases are key enzymes attributed to collagen degradation, which results in impaired skin structural integrity. Collagen is the main structural protein in the extracellular matrix constituting not only skin but also cartilage, bone, and other connective tissue. It is also involved in a wound-healing process by contributing to cellular migration and new tissue development [12]. Collagenases are zinc-containing proteinases that are a type of matrix metalloproteinases (MMPs). MMP-1 can trigger the breakdown of type I, II and III collagens, which are found abundantly in the dermis. On the other hand, MMP-2 is responsible for the degeneration of not only collagen type I–III but also type IV and VII, which mostly reside in the dermal–epidermal junction [13]. UV-induced ROS can increase collagenase activities via the MAPK pathway [5,7]. When the ROS chronically and cumulatively induce the activities of collagenases, skin collagens can become depleted over time, leading to wrinkle formation, aging skin, and delay of wound healing [14].

In addition to healthy skin, hair is another aesthetic concern for overall appearance. Androgenic alopecia (AGA) is the most common hair loss affecting both men and women. Early onset appears in the teens; however, most cases occur later in life. It affects 50% of males by age 50 years and up to 70% by 70 years [15,16]. AGA is a genetic disorder of dysfunctional androgens caused by the inordinate induction of 5 $\alpha$ -reductase in hair follicles [17]. This results in an acceleration of excessively converting testosterone to the higher potent dihydrotestosterones, which then trigger the development of AGA pathogenesis leading to hair loss and pattern baldness [18,19].

Nowadays, treatments addressing skin hyperpigmentation, wrinkles, and hair loss mostly involve chemically synthetic compounds that often lead to undesired effects. Tyrosinase inhibitor hydroquinone is a depigmenting agent used to lighten darkened skin; however, it causes dermatitis, edema, and ochronotic condition [20]. Skin aging remedies involving topical hydroxyl acid to shed old sun-damaged epidermal layers, topical retinoids to improve fine lines, and directly injecting collagen to reduce wrinkles can lead to hyperpigmentation, inflammation, and bacterial infection [21,22]. For hair loss, potassium channel opener minoxidil and 5 $\alpha$ -reductase inhibitor finasteride are the only two drugs that are currently approved by the United States Food and Drug Administration (US FDA) for AGA [2]. However, minoxidil causes erythema, dizziness, and tachycardia, while finasteride leads to erectile dysfunction, gynecomastia, and severe myopathy. Therefore, there are rising demands for natural products as alternatives to chemically synthetic ingredients in skin and hair treatments. In addition, increasing awareness of the harmful impacts of synthetic chemicals on the environment is another attribute accelerating the growth of incorporating natural elements in cosmeceuticals.

Horsetails (*Equisetum*) are one of the oldest vascular plants that have existed prior to the continental drift as indicated by fossil records. *Equisetum* comprises over thirty species, and due to the adaptability to distinct climates, their distribution spans from the equator to the northern hemisphere [23,24]. Horsetails are also known as the most ancient remedies in several countries. *E. arvense* L., native to north America and Europe, is the most investigated horsetail due to the long-standing traditional usage. Its medicinal values, particularly for skin and hair care, have been recorded not only in folklores but also in scientific literature. Traditionally, it is used to treat poorly healing wounds, hair loss, brittle nails, bone fractures, diuretic, and rheumatic diseases, potentially due to the species' high silica, total phenolics, flavonoids, phytosterols, and saponins [23,25,26]. In cosmeceuticals, *E. arvense* extracts are recognized as a skin collagen-promoting agent,

anti-aging agent, and hair-promoting ingredient. Mixtures of *E. arvense* extracts with other herbs in dietary supplements and topical formulations are known to promote healthy hair follicles and hair growth. A placebo-controlled, single-blind, clinical instrumental study showed that herbal formulations containing *E. arvense* extracts helped prevent hair from falling out and reduced hair loss [27]. In clinical trials, topical phytotherapy combining *E. arvense* extracts with other herbal extracts showed benefits to brittle nail disorder. Ointment containing *E. arvense* (3%) showed wound-healing effects [28]. Other clinical trials reported the efficacies of *E. arvense* for benign prostate hyperplasia and chronic musculoskeletal pain [29]. Additionally, the diuretic effect of *E. arvense* was superior to control but equivalent to hydrochlorothiazide [30].

On the other hand, *E. debile* Roxb. Ex Vaucher, a species native to tropical Asia, is a far less studied horsetail [24]. In Thailand, it is distributed throughout the northern highland with typical hills up to 500 m. Traditionally, the local hill tribe people prepare decoctions of *E. debile* for strengthening hair, treating urinary incontinence, kidney stones and back-pain. Poultices of *E. debile* are used for healing warts, wounds, bone fractures and joint pain. The similarity of morphological taxonomy, genetic relevance, and traditional usages between the two species suggest that *E. debile* may possess comparative phytochemicals and pharmacological activities to *E. arvense*. *E. debile* may possibly be a tropical counterpart to a temperate *E. arvense* for the species' medicinal benefits. Horsetail-based commercial products are mostly derived from the *E. arvense* due to not only being highly supported by scientific studies more often than other horsetail species but also being recognized and established as an herbal medicine in the monograph of European Pharmacopoeia 8th edition [31]. Conversely, *E. debile* is still underexploited despite potential medicinal values. *E. debile* has been studied for total phenolic content, antioxidant activities, antibacterial activities, 5 $\alpha$ -reductase inhibition, interleukin 6 (IL-6) secretion inhibition, evaluation of membrane irritation, cytotoxicity, and phytochemical isolations of pinocembrin, chrysin,  $\beta$ -sitosterol, flavonoid glycoside, fatty acids, and megastigmane diglucoside [32–34]. However, previous reports were limited to the investigation of extracts obtained from macerations.

Horsetail plants are known to accumulate considerable amounts of silicon (Si) [35]. Si is found in various tissues of the human body and present in 1–10 parts per million in hair and nails [36]. Oral intake of choline-stabilized orthosilicic acid (a bioavailable form of silicon) resulted in a positive effect on skin surface and skin mechanical properties as well as on brittleness of hair and nails during a 20-week randomized, placebo-controlled double-blind study of women with photodamaged skin [37]. However, determination of Si content is mostly reported for *E. arvense*.

Therefore, this study aims to demonstrate the application of a sequential extraction technique using a series of solvents with increasing polarities to acquire *E. debile* semi-purified fractions. The obtained extracts were then investigated for silicon, phenolics, and cosmeceutical effects by assessing the *in vitro* inhibition activities against tyrosinase, collagenases, and 5 $\alpha$ -reductase. This is the first report that compares *E. debile* crude extract and semi-purified fractions for bioactivities relating to cosmeceutical applications. Additionally, several factors including pH, temperature, light, oxygen, metal ions, and other chemical constituents could influence degradations of bioactive compounds. Therefore, the present study also aims to evaluate stability profiles of cosmeceutical bioactivities from *E. debile* extracts during storage.

## 2. Materials and Methods

### 2.1. Chemicals and Reagents

All chemicals and solvents used in this study were analytical grade. Folin–Ciocalteu reagent, gallic acid, kojic acid, 1,10-phenanthroline, (-)-epigallocatechin 3-gallate (EGCG), finasteride, L-3,4-dihydroxyphenylalanine (L-DOPA), and tyrosinase were purchased from Sigma-Aldrich (St. Louis, MO, USA). Ethanol, hexane, dichloromethane, ethyl acetate, and methanol were purchased from Labscan (Dublin, Ireland). EnzChek Gelatinase/Collagenase assay kit (E-12055) was purchased from Molecular-Probes (Eugene, OR, USA).

### 2.2. Plant Materials

*E. debile* plant materials were collected from field plots around the highland area of the Mae-Na Agricultural station, Chiang Dao District, Chiang Mai Province in northern Thailand during October to December 2016 following WHO guidelines on good collection practices for medicinal plants [38] and EMA guidelines on collection for starting materials of herbal origin [39]. Plant samples were authenticated by the Highland Research and Development Institute (public organization Chiang Mai, Thailand). The plant specimen was maintained under the voucher number 0023246 at the herbarium facility, Faculty of Pharmacy, Chiang Mai University, Chiang Mai, Thailand. Only the plant aerial parts were used in this study. The harvested plant samples were thoroughly washed under running tap water to remove soil, dust, and rock particles and then oven dried at 50 °C for 8 h. The dried plants were cut into small pieces and pulverized to a coarse powder using a heavy-duty blender prior to the extraction procedure.

### 2.3. Plant Extraction Procedures

#### 2.3.1. Preparation of Crude Extracts

Ethanol is a commonly used solvent in botanical extraction, which is partly due to safety and extractability for both non-polar and polar phytochemicals. It is also a well-known solvent for polyphenol extraction and safe for human consumption. Therefore, ethanol was used to obtain crude extract (CE) in the present study. The dried *E. debile* coarse powder was immersed in 95% ethanol (1 kg dried plant per 10 L 95% ethanol). The maceration was performed at room temperature for three days in a closed vessel with occasional agitation and repeated three times. The supernatant of the macerated mixture was collected by a vacuum filtration step using Whatman filter paper grade 1 (particle retention (liquid) at 11 µm and diameter of 90 mm) to remove plant tissue residues. Total filtrate was then dried by using a rotary evaporator under reduced pressure to produce a crude extract (CE). The ethanolic crude extracts were stored at 4 °C until further isolation of semi-purified fractions.

#### 2.3.2. Isolation of Semi-Purified Fractions by Solvent–Solvent Partitioning Method

Prior to the fractioning process, CE was resuspended by methanol rather than ethanol. This is because methanol is immiscible with hexane, which was the first non-polar solvent in the partitioning process. Additionally, methanol has similar extractabilities to ethanol to recovering high amounts of phenolics and flavonoids [40–42].

The CE samples were submitted to a partitioning process modified from previous methods [43,44] by using various organic solvents to sequentially extract the compounds from a low to high range of polarities. This technique partitioned CE by polarities of compounds into four fractions of hexane (HF), dichloromethane (DF), ethyl acetate (EF), and methanol (MF), as shown in Figure 1. The experiment was performed in triplicate, and the percentage yield for each fraction was calculated according to a following equation:

$$\% \text{yield} = \text{dry weight of semi-purified fraction} / \text{dry weight of crude extract} \times 100$$

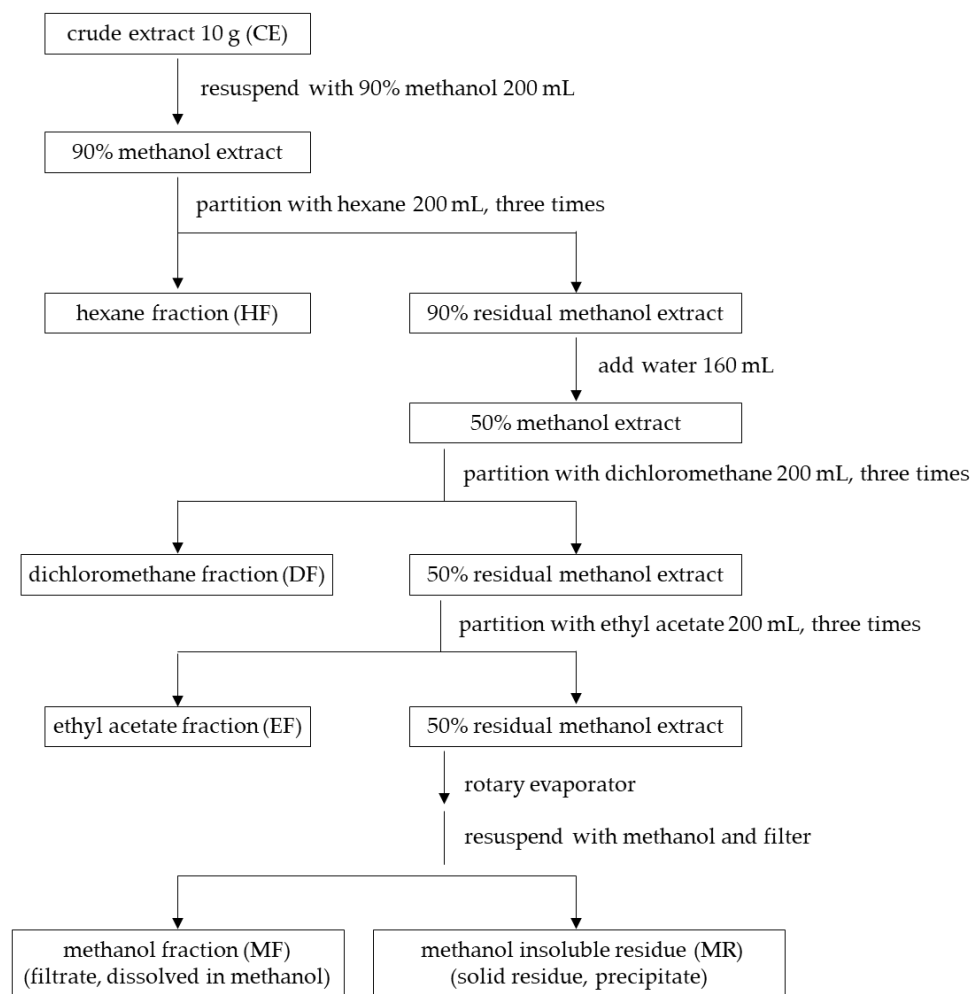


**Figure 1.** Partitioning of *E. debile* crude extract (CE) to obtain fractions hexane (HF), dichloromethane (DF), ethyl acetate (EF), methanol (MF), and methanol insoluble residue (MR).

#### 2.4. Determination of Silicon (Si)

Plant extracts (30 mg) were re-suspended in deionized water (8 mL) using a sonicator at 60 °C for five minutes. The solutions of crude extract and hexane fraction were filtered by 110 nm filter paper (WINTTECH). The solutions of dichloromethane, ethyl acetate and methanol fractions were filtered by a 0.22 µM filter membrane (Nylon). The volumes of all filtrates were adjusted to 10 mL and then subjected to an acid digestion process prior to silicon analysis. Samples were submitted to the Central Science Laboratory, Faculty of Sciences, Chiang Mai University (Chiang Mai, Thailand) for a silicon analysis procedure. The measurements of silicon were determined by inductively coupled plasma–optical emission (ICP-OES) spectrometer (Perkin Elmer Optima 7300 DV) with the operational system (parameter and conditions) described in Table 1.

**Table 1.** Operational parameters of inductively coupled plasma–optical emission (ICP–OES) spectrometer for silicon (Si) determination from *E. debile* extracts.

Instrument Parameters	Operational Conditions
ICP RF power (w)	1300
Plasma gas (L/min)	15
Auxiliary gas (L/min)	0.2
Nebulizer gas (L/min)	0.8
Viewing type	Axial
Read delay (seconds)	15
Replicates	3
Sample flow rate (mL/min)	1.5
Flush time (seconds)	25
Wavelength (nm)	Si 212.412

### 2.5. Determination of Total Phenolic Content by Folin–Ciocalteu Assay

Total phenolic contents of *E. debile* extracts were investigated using the Folin–Ciocalteu method. Gallic acid was used as a standard for a quantification of total phenolic content. The gallic acid was dissolved in 95% ethanol, and the solutions were prepared in various concentrations to construct a standard curve. A volume of 300 µL of gallic acid at each concentration was mixed with 1.5 mL of Folin–Ciocalteu reagent (10% *v/v*) and kept at room temperature in the dark for three minutes, which was followed by an addition of 1.2 mL Na<sub>2</sub>CO<sub>3</sub> (75 mg/mL). Incubation of the reactions continued for 30 min. The sample absorbance was measured at 731 nm by using a spectrophotometer (Beckman Coulter DTX880, Fullerton, CA, USA). The experiment was performed in triplicate for each gallic acid concentration. For plant samples, the procedure was also carried out similarly to gallic acid. All dried extracts were re-suspended by 95% ethanol prior to mixing with Folin–Ciocalteu reagent. Total phenolic content of plant samples was expressed as gallic acid equivalents (GAE) by extrapolating its corrected absorbance against the gallic acid calibration curve.

### 2.6. Determination of Tyrosinase Inhibition (Skin-Whitening Activity)

Melanin is a brown pigment that plays a major role to induce a darkened complexion of skin appearance. Lowering melanin production via an inhibition of tyrosinase activity has been recognized to brighten a dark skin shade, leading to a lighter or whitening appearance. Therefore, a skin-whitening property of *E. debile* extracts was investigated via the inhibitory capacity against the activity of tyrosinase using a dopachrome 96-well plate method with some modifications [45]. Briefly, tyrosinase accelerated an enzymatic reaction to convert L-DOPA substrate to brown pigment products (pheomelanin and eumelanin) that were quantified using a UV-Vis spectrophotometer with an absorbance at 492 nm. Before testing, the *E. debile* extracts were re-suspended in 50 mM phosphate buffer pH 6.8. The reaction was a mixture of 50 µL L-DOPA (15 mM in 50 mM phosphate buffer pH 6.8) and 50 µL plant extract, which was followed by an addition of 50 µL tyrosinase (100 units/mL). The experiment was carried out in a 96-well microplate, and the absorbance was measured before and after an activation of tyrosinase activity. The incubation condition was maintained at 37 °C (to mimic human skin temperature) for 60 min to initiate an enzymatic reaction. The following equation was used to compute the percent tyrosinase inhibition [32]:

$$\% \text{ inhibition} = [(A - B) - (C - D)] / (A - B) \times 100,$$

where A is an absorbance of plant samples before an enzymatic incubation with B as a blank. C is an absorbance of plant samples after the incubation with D as a blank.

Kojic acid, a well-known tyrosinase inhibitor, was used as a standard. Kojic acid solution was prepared in various concentrations to obtain a calibration curve. The enzymatic reaction of kojic acid was performed similarly to the plant samples described above. The

inhibitory capacity of *E. debile* against tyrosinase activity was expressed as KAE values (mg kojic acid equivalent per gram plant sample) using an equation derived from a kojic acid calibration curve and IC<sub>50</sub> value which is the inhibitor concentration leading to 50% activity loss.

### 2.7. Determination of Collagenase Inhibition (Anti-Wrinkle Activity)

Excessive and prolonged oxidative stress can promote the skin aging process associated with an occurrence of wrinkles [46]. Additionally, during a skin injury, dermal fibroblasts engage cell-repairing mechanisms to restore skin integrity. Fibroblast cells play a key role in the production of collagens and other proteins that constitute the dermis and preserve skin function [47]. Therefore, overactivated collagenase caused by oxidative stress could degenerate collagens, leading to wrinkle formation and inhibiting the wound-healing process. An inhibition of collagenase activity was proved to delay the loss of collagen fibers. It is also associated with the potential prevention of skin damage prior to injury. Collagenase inhibition could slow skin deterioration and aging processes, thereby reducing the formation of wrinkles. Thus, this study examined the anti-wrinkle activities of *E. debile* extracts via the inhibitions of collagenase activities.

Inhibition assays of MMP-1 and MMP-2 collagenase were conducted by using the EnzChek Gelatinase/Collagenase assay kit (E-12055). The DQ collagen 1 was used as a substrate for MMP-1, and the DQ gelatin was used as a substrate for MMP-2. The experiments were performed according to the company's instruction with some modifications. Briefly, *E. debile* extracts were re-suspended prior to being tested. The testing solution was a mixture of 20 µL of DQ substrates (12.5 mg/mL) and 80 µL of plant extract, which was followed by the addition of collagenase (0.2 units/mL). The experiment was carried out in a 96-well plate and incubated in the dark at room temperature for 90 min. Fluorescent intensity of the enzymatic reaction was measured at excitation/emission of 485/538 nm by a microplate reader. A well-known collagenase inhibitor, 1,10-phenanthroline, was used as a standard. EGCG was used as a positive control. The following equation was used to compute the percent collagenase inhibition [48,49]:

$$\% \text{ collagenase inhibition} = [(A - B) - (C - D)] / (A - B) \times 100,$$

where A is a reaction with the presence of enzyme but without a testing sample, B is a reaction without both a testing sample and enzyme, C is a reaction with the presence of both a testing sample and enzyme, and D is a reaction with the presence of a testing sample but without enzyme. Additionally, an inhibitory capacity of *E. debile* against collagenase activity was expressed as an IC<sub>50</sub> value.

### 2.8. Determination of 5α-Reductase Inhibition (Anti-Hair Loss Activity)

A potential mechanism underlying the anti-hair loss activity of *E. debile* extracts was investigated through its association with anti-androgenic activity via the inhibitory effect against steroid 5α-reductase. The inhibitory capacities were determined by measuring the remaining testosterone substrate using high-performance liquid chromatography (HPLC) after a forced termination of an enzymatic reaction. The enzymatic preparation and inhibitory assay of 5α-reductase were conducted according to a previous method with some modifications [50] described below.

### 2.8.1. Preparation of Rat Microsomal Suspension

The enzyme source used in the *in vitro* inhibition assay of 5 $\alpha$ -reductase activity was derived from rat microsomal suspensions obtained from the donated, unused livers of two male Wistar rats in the control group of an unrelated study by Khat-udomkiri et al., 2020 [51], in which all experiment protocols were approved by the Research Animal Care and Use Ethical Committee, Faculty of Pharmacy, Chiang Mai University, Thailand (Ethics approval no. 04/2015), in compliance with the National Institutes of Health and ARRIVE guidelines for the care and treatment of animals. Unused parts of the donated livers were homogenized in a solution (0.32 M sucrose and 1 mM dithiothreitol in 0.02 M phosphate buffer at pH 6.5) at a ratio between liver mass and solution of 1:5. The resulting homogenized liver mixture was centrifuged at 1500  $\times$  g at 0  $^{\circ}$ C for 20 min. The retrieved supernatant was then centrifuged at 4500  $\times$  g twice at 0  $^{\circ}$ C for 30 min. The last two supernatants were combined to produce the rat microsomal suspension as a source of 5 $\alpha$ -reductase. The suspension quality control was assessed by estimating protein content using the previously reported method [52]. All supernatants were maintained at 50  $^{\circ}$ C until used in an enzymatic reaction.

### 2.8.2. Inhibitory Assay of 5 $\alpha$ -Reductase Activities

*E. debile* extracts were re-suspended using either 50% ethanol or dimethyl sulfoxide: ethanol (1:1) to produce a final concentration of 1 mg/mL prior to being tested for inhibitory activities of 5 $\alpha$ -reductase. The testing mixtures were prepared by combining 0.2 mL of a plant sample, 1 mL of phosphate buffer (0.02 mM, pH 6.5), 0.3 mL of testosterone substrate (500 ppm) in 50% ethanol, and 1 mL of a rat microsomal suspension (4 mg protein/mL). The enzymatic reactions were activated by an addition of 0.5 mL of NADPH (0.77 mg/mL), which was followed by an incubation in a water bath at 37  $^{\circ}$ C for 30 min. The reactions were immediately stopped by adding 5.0 mL dichloromethane. Propyl p-hydroxybenzoate (100 ppm in 50% ethanol) was added to the sample as an HPLC internal standard. The amount of remaining testosterone substrate in the terminated enzymatic reaction was determined using the HPLC system (Agilent Technologies, Santa Clara, CA, USA) equipped with the analytical reversed phase column Shodex C18-4E column (250  $\times$  4.6 mm, 5  $\mu$ m particle size) with the analysis conditions of column temperature at 40  $^{\circ}$ C, a mobile phase of methanol:deionized water (65:35), a flow rate at 1 mL/min, an injection volume of 10  $\mu$ L, and a detection at 242 nm.

Negative and positive controls were prepared for computing the inhibitory capacity of plant samples. The reaction mixtures for both controls were assembled and carried out similarly to the plant samples described above. The negative control was an enzymatic reaction without any inhibition (0% inhibition). It was prepared by substituting the plant sample with 50% ethanol. The positive control represented 100% inhibition of 5 $\alpha$ -reductase activity. It was prepared by using dichloromethane to denature any protein or enzyme from a microsomal suspension preceding an initiation of the enzymatic reaction. The % inhibition was calculated by peak area ratio (R) of the remaining testosterone and internal standard using the following equation [50]:

$$\% \text{ inhibition} = [(R_{\text{sample}} - R_{\text{negative}}) / (R_{\text{positive}} - R_{\text{negative}})] \times 100$$

In this study, finasteride was used as a commercial standard in order to compare an inhibitory capacity of the *E. debile* extracts. Finasteride was prepared in various concentrations from 0.1 to 0.5  $\mu$ M to produce a standard curve. The inhibitory capacities of all plant extracts against 5 $\alpha$ -reductase were expressed as finasteride equivalent 5 $\alpha$ -reductase inhibitory activity (FEA) values, representing a unit of mg finasteride equivalent per 1 g plant extract.

### 2.9. In Vitro Cytotoxicity Test Using MTT Assay

Cell viability was assessed by a modified method [53] on human normal skin fibroblast (SF-TY) cell line (JCRB0075). Briefly, after the treatment with *E. debile* extracts, the viability of SF-TY cells was determined by 3-(4,5-dimethylthiazol-2-yl)-2,5-diphenyl tetrazolium bromide (MTT-Sigma-Aldrich, St. Louis, MO, USA) assay. The MTT is reduced by mitochondrial dehydrogenases to the water-insoluble purple compound formazan, depending on cell viability. Cells were maintained in Dulbecco's Modified Essential Medium (DMEM) supplemented with 10% fetal bovine serum (FBS) and  $1 \times$  penicillin–streptomycin. Then, 100  $\mu$ L of cells ( $8 \times 10^4$  cells/mL) was seeded in 96-well plates and incubated at 37 °C and 5% CO<sub>2</sub> for 24 h. After, cells were treated with 100  $\mu$ L of *E. debile* extracts with the concentration obtained from the bioactivity results, which covered IC<sub>50</sub> values at 1, 2.5, 5, 7.5 and 10 mg/mL. Plates were then incubated at 37 °C and 5% CO<sub>2</sub> for 24 h. After the incubation, plates were washed with PBS; then, 20  $\mu$ L of MTT solution (5 mg/mL in PBS) was added to each well and incubated at 37 °C for 3 h. The medium was discarded, and formazan crystals were suspended with 100  $\mu$ L of dimethyl sulfoxide (DMSO-Sigma-Aldrich, St. Louis, MO, USA). The absorbance was measured at 570 nm and percentages of viable cells and IC<sub>50</sub> were calculated using the following equation [54]:

$$\% \text{ cell viability} = (\text{Absorbances}_{\text{Tests}} / \text{Absorbances}_{\text{Control}}) \times 100,$$

where Absorbances<sub>Control</sub> is the absorbance of cells treated with 1% DMSO and Absorbances<sub>Tests</sub> is the absorbance of cells treated with plant extract.

### 2.10. Stability Study

*E. debile* crude extract and semi-purified fractions were stored in tight container closures and protected from light. All samples were then kept in a stability cabinet under an accelerated storage condition at 40 °C for three months to study extract stability profiles. The degradation of some phytochemicals could affect the cosmeceutical potentials of the extracts; therefore, the extract stability was determined by comparing the *in vitro* inhibitory activities against tyrosinase, collagenases, and 5 $\alpha$ -reductase between month 0 and month 3.

### 2.11. Statistical Analysis

Significant differences were evaluated by Student's *t*-test and one-way ANOVA followed by post hoc tests using GraphPad Prism v8.0 (GraphPad, La Jolla, CA, USA) and SPSS 17.0 (SPSS Inc., Chicago, IL, USA).

## 3. Results

### 3.1. *E. debile* Crude Extract and Semi-Purified Fractions

The extract yields and physical appearances were distinct among the fractions (Figures 2 and 3). HF had the highest yield ( $43.64 \pm 1.80\%$ ), which was followed by DF ( $24.03 \pm 1.72\%$ ), MR ( $11.25 \pm 6.77\%$ ), MF ( $10.50 \pm 0.52\%$ ), and EF ( $3.88 \pm 0.27\%$ ). CE was blackish brown, highly sticky, and semi-solid. The appearances of HF and DF were both blackish greens and highly viscous. On the other hand, EF was deep brown and sticky. MF was golden brown and slightly sticky, and MR was creamy white and a salt-like coarse powder. Taken together, this suggests that the solvent–solvent partitioning method allowed the isolation of the semi-purified fractions from crude extract, depending on the constituent polarity indices.

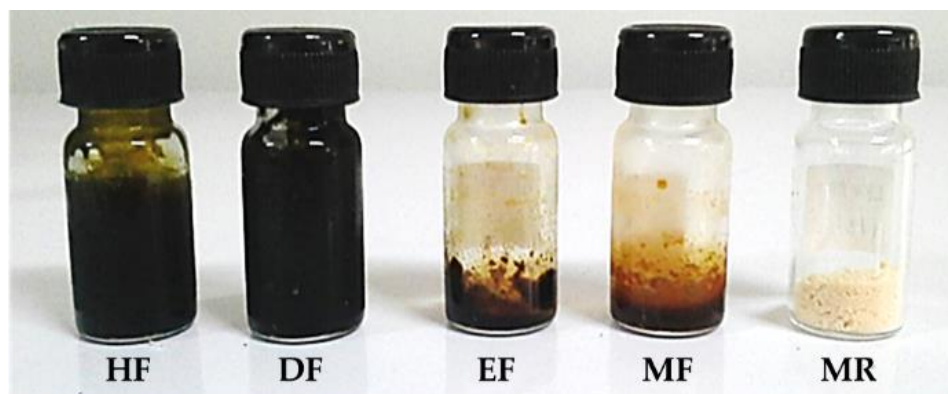


**Figure 2.** Physical appearances of *E. debile* hexane fraction (HF), dichloromethane fraction (DF), ethyl acetate fraction (EF), methanol fraction (MF), and methanol insoluble residue (MR).

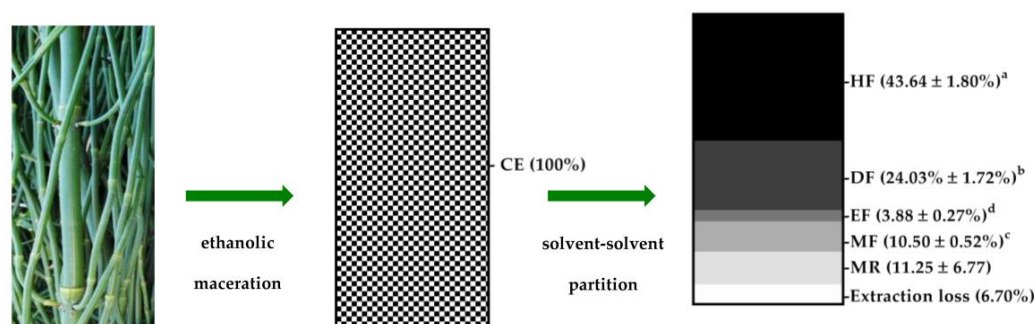


**Figure 3.** *E. debile* crude extract (CE) sequentially partitioned into semi-purified hexane fraction (HF), dichloromethane fraction (DF), ethyl acetate fraction (EF), methanol fraction (MF), and methanol insoluble residue (MR). The % yield is a ratio of fraction weight and crude extract weight. All data are presented as mean  $\pm$  SD of three independent experiments. Superscript letters (a, b, c, and d) indicate significant differences of means between the groups based on Tukey's HSD one-way ANOVA ( $p$ -value  $<$  0.05).

### 3.2. Determination of Silicon Contents

Some portions of silicon presented in the plant samples were extractable by ethanolic maceration and a sequential partitioning with various solvents (Table 2). The extractable silicon varied between 0.012 and 0.033% depending on the extraction methods and solvents. CE yielded the highest extractable silicon (0.033%). The yields were similar among HF (0.022%), DF (0.018%), and EF (0.019%). The least silicon amount was found in MF (0.012%). The silicon amount combined from all fractions yielded two-fold higher than the crude extract, which indicates that the silicon element in *E. debile* samples might be presented in various complex forms, leading to the variation of extractability. Therefore, the silicon components of *E. debile* might possess some solubility ranges.

Despite Si being linked to cosmeceutical benefits of horsetail for skin, hair, and nail, it was not related to the observed inhibition activities against tyrosinase ( $R^2 = 0.0313$  and regression  $p$ -value = 0.7758), 5 $\alpha$ -reductase ( $R^2 = 0.1119$  and regression  $p$ -value = 0.5821), MMP-1 ( $R^2 = 0.2381$  and regression  $p$ -value = 0.4044), and MMP-2 ( $R^2 = 0.1913$  and regression  $p$ -value = 0.4613) of *E. debile* extracts, as shown in Figure 4.

**Table 2.** Extractable silicon contents from *E. debile* tissues.

Extracts	Extract Mass (mg)	Extractable Si (mg $\pm$ SD)	% Extractable Si $\pm$ SD
CE	32.6	0.0109 $\pm$ 0.00011	0.033 $\pm$ 0.0003 <sup>a,b</sup>
<sup>i</sup> HF	35.1	0.0078 $\pm$ 0.00009	0.022 $\pm$ 0.0003 <sup>b</sup>
<sup>ii</sup> DF	33.6	0.0060 $\pm$ 0.00004	0.018 $\pm$ 0.0001 <sup>b</sup>
<sup>iii</sup> EF	31.0	0.0059 $\pm$ 0.00004	0.019 $\pm$ 0.0002 <sup>b</sup>
<sup>iv</sup> MF	32.9	0.0041 $\pm$ 0.00007	0.012 $\pm$ 0.0001 <sup>b</sup>
<sup>v</sup> MR	32.6	0.0012 $\pm$ 0.00003	0.004 $\pm$ 0.0001 <sup>c,b</sup>

<sup>i-v</sup> Successive partition of crude extract (CE) (10.45  $\pm$  1.20 g) into hexane fraction (HF), dichloromethane fraction (DF), ethyl acetate fraction (EF), methanol fraction (MF), and methanol insoluble residue (MR). Superscript letters indicate significant differences between the groups based on Tukey's HSD one-way ANOVA ( $p$ -value < 0.05).

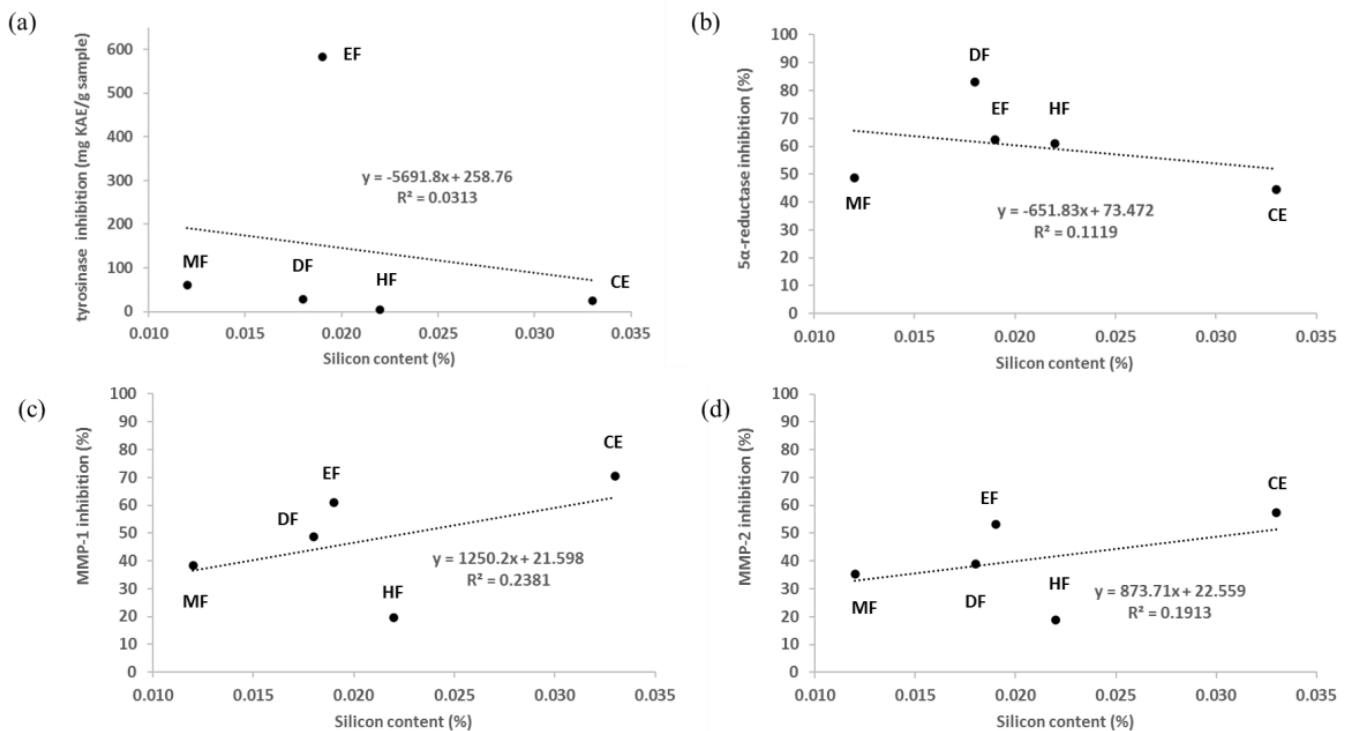


**Figure 4.** Relative scatter plot of silicon content and inhibition activities of crude extract (CE), hexane fraction (HF), dichloromethane fraction (DF), ethyl acetate fraction (EF), and methanol fraction (MF); (a) anti-tyrosinase activity (regression  $p$ -value = 0.7758); (b) anti-5 $\alpha$ -reductase activity (regression  $p$ -value = 0.5821); (c) anti MMP-1 activity (regression  $p$ -value = 0.4044); and (d) anti MMP-2 activity (regression  $p$ -value = 0.4613).

### 3.3. Determination of Total Phenolic Contents

Figure 5 shows that TPC were affected by solvents and extraction methods. The regression equation derived from the gallic acid calibration curve was  $y = 0.0912x + 0.0091$ ,  $R^2 = 0.9992$  and used to compute GAE values. The highest TPC was obtained from EF, which was eleven-fold higher than the lowest, and comparative TPC values were obtained from DF and HF. The TPC values of *E. debile* extracts were ranked by GAE as the following: EF (39.24  $\pm$  0.72 mg GAE/g extract), CE (17.89  $\pm$  5.10 mg GAE/g extract), MF (9.70  $\pm$  0.21 mg GAE/g extract), DF (4.37  $\pm$  0.08 mg GAE/g extract), and HF (3.53  $\pm$  0.80 mg GAE/g extract). The association between TPC and the inhibition activities against tyrosinase, 5 $\alpha$ -reductase, MMP-1, and MMP-2 of *E. debile* extracts was shown in Figure 6.

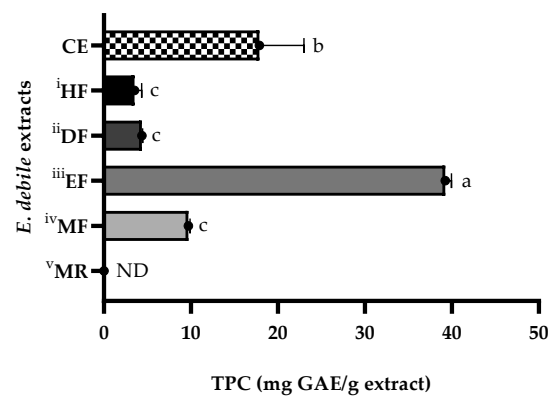


**Figure 5.** Total phenolic contents (TPC) of *E. debile* extracts. <sup>i–v</sup> Successive partition of crude extract (CE) ( $10.45 \pm 1.20$  g) into hexane fraction (HF), dichloromethane fraction (DF), ethyl acetate fraction (EF), methanol fraction (MF), and methanol insoluble residue (MR). All data are presented as mean  $\pm$  SD of triplicates. Total phenolic contents were expressed as GAE (gallic acid equivalents). ND indicates not detected. Letters (a, b, and c) indicate significant differences of means between the groups based on Tukey's HSD one-way ANOVA ( $p$ -value  $< 0.05$ ).

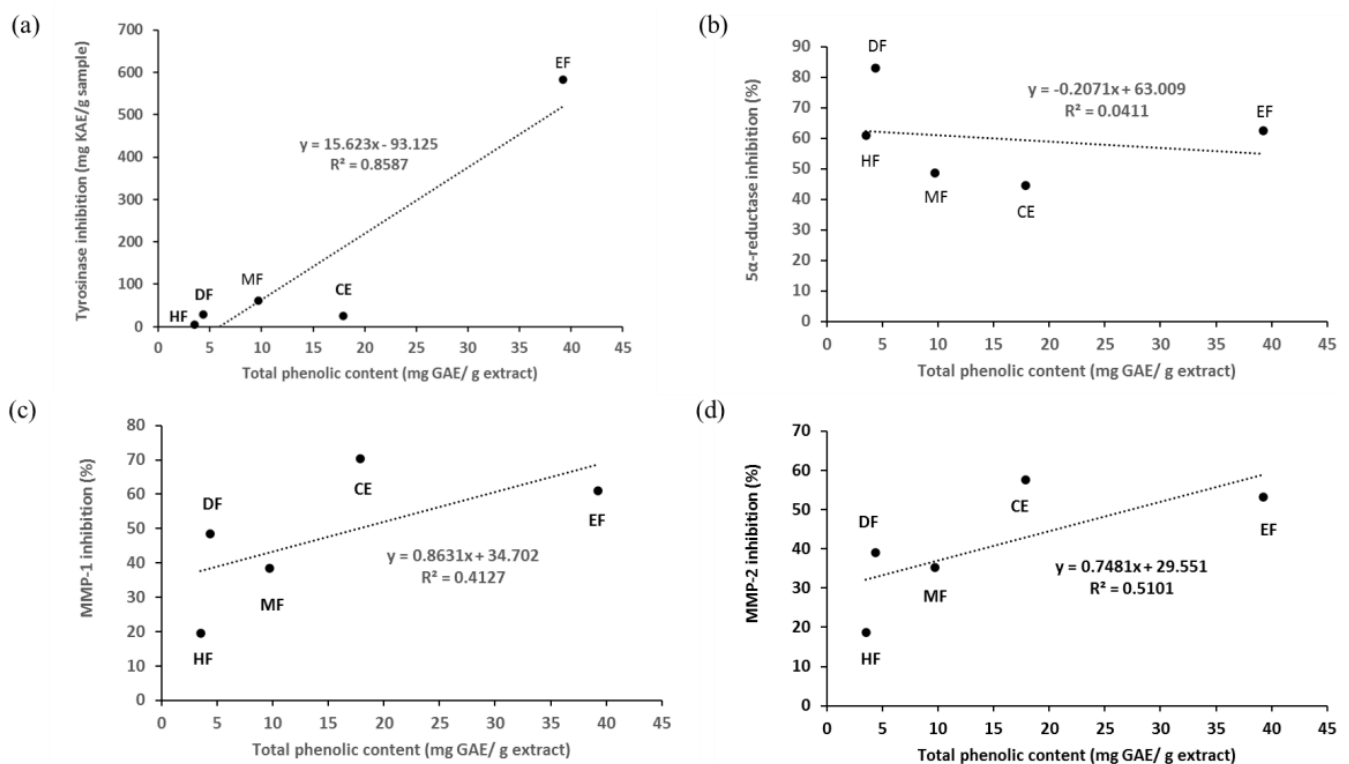


**Figure 6.** Relative scatter plot of total phenolic content and inhibition activities of crude extract (CE), hexane fraction (HF), dichloromethane fraction (DF), ethyl acetate fraction (EF), and methanol fraction (MF); (a) anti-tyrosinase activity (regression  $p$ -value = 0.0236); (b) anti-5 $\alpha$ -reductase activity (regression  $p$ -value = 0.7437); (c) anti MMP-1 activity (regression  $p$ -value = 0.2424); and (d) anti MMP-2 activity (regression  $p$ -value = 0.1753).

### 3.4. Skin-Whitening Activities of *E. debile* Extracts via the Inhibition of Tyrosinase Enzyme

Figure 7 and Table 3 demonstrate that the tyrosinase inhibitory capacities of *E. debile* extracts were influenced by the extraction methods and solvents. The regression equation derived from the kojic acid calibration curve was  $y = 8.8622x + 1.9838$ ,  $R^2 = 0.998$  and used to compute KAE values. The highest anti-tyrosinase activity was from EF, which was higher than the lowest activity from HF by 114-fold KAE values. HF and DF exhibited similar

potency of inhibition to CE; however, these three extracts exerted lower activities than that of MF. Anti-tyrosinase activities were ranked by KAE and IC<sub>50</sub> values as the following: EF, MF, DF, CE, and HF. This suggests that the partitioning extraction by ethyl acetate was able to isolate strong tyrosinase inhibitors from *E. debile* crude extract.

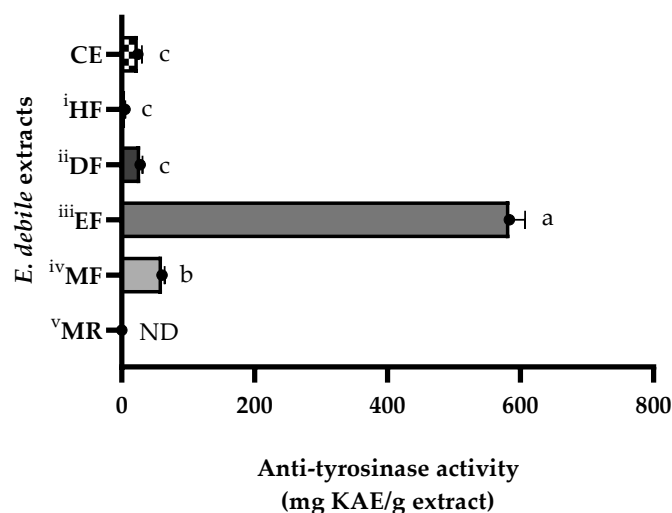


**Figure 7.** Anti-tyrosinase activities of *E. debile* extracts. <sup>i–v</sup> Successive partition of crude extract (CE) (10.45 ± 1.20 g) into hexane fraction (HF), dichloromethane fraction (DF), ethyl acetate fraction (EF), methanol fraction (MF), and methanol insoluble residue (MR). All data are presented as mean ± SD of triplicates. Anti-tyrosinase activities were expressed as KAE (kojic acid equivalents). ND indicates not detected. Letters (a, b, and c) indicate significant differences of means between the groups based on Tukey’s HSD one-way ANOVA (*p*-value < 0.05).

**Table 3.** Anti-tyrosinase and anti-5α-reductase activities of *E. debile* extracts.

Extracts	Anti-Tyrosinase IC <sub>50</sub> (mg/mL)	Anti-5α-Reductase FEA (mg Finasteride/g Extract)
CE	3.78 ± 0.24 <sup>b</sup>	0.83 ± 0.01 <sup>c</sup>
<sup>i</sup> HF	5.96 ± 0.11 <sup>a</sup>	1.10 ± 0.01 <sup>b</sup>
<sup>ii</sup> DF	3.54 ± 0.10 <sup>b</sup>	1.48 ± 0.06 <sup>a</sup>
<sup>iii</sup> EF	0.47 ± 0.12 <sup>d</sup>	1.13 ± 0.01 <sup>b</sup>
<sup>iv</sup> MF	2.25 ± 0.08 <sup>c</sup>	0.90 ± 0.06 <sup>c</sup>
<sup>v</sup> MR	ND	0.87 ± 0.01 <sup>c</sup>

<sup>i–v</sup> Successive partition of crude extract (CE) (10.45 ± 1.20 g) into hexane fraction (HF), dichloromethane fraction (DF), ethyl acetate fraction (EF), methanol fraction (MF), and methanol insoluble residue (MR). All data are presented as mean ± SD of triplicates. IC<sub>50</sub> is the half maximal inhibitory concentration. FEA is the finasteride equivalent 5α-reductase inhibitory activity. ND indicates not detected. Superscript letters (a, b, c, and d) within the same column indicate significant differences of means between the groups based on Tukey’s HSD one-way ANOVA (*p*-value < 0.05).

### 3.5. Anti-Wrinkle Activities of *E. debile* Extracts via the Inhibition of Collagenase Enzymes

Figure 8 demonstrates that the collagenase inhibitory capacities of *E. debile* extracts varied by the extraction methods and solvents. All extracts except MR exhibited dose-dependent inhibitions against both MMP-1 and MMP-2 collagenases. In addition, the inhibition patterns of MMP-1 were strongly consistent with MMP-2. The anti-collagenase activities were ranked by the IC<sub>50</sub> values of both collagenases as the following: CE, EF, DF, MF, and HF. The MR showed no detectable activities of collagenase inhibitions. EF exerted the highest inhibitions among all fractions, which were higher than the lowest activities from HF by 3.1-fold of the IC<sub>50</sub> MMP-1 and 2.8-fold of the IC<sub>50</sub> MMP-2. The EF also contained the richest total phenolic contents.

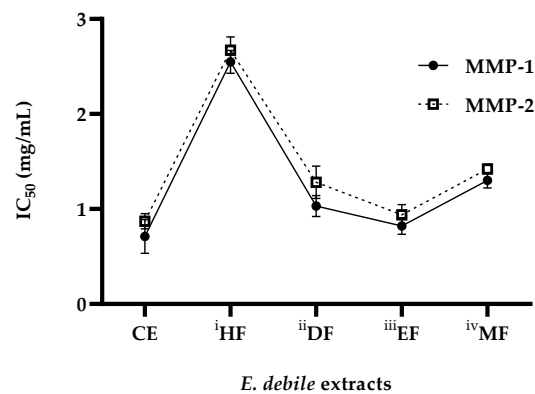


**Figure 8.** Anti-collagenase activities of *E. debile* extracts. <sup>i–v</sup> Successive partition of crude extract (CE) ( $10.45 \pm 1.20$  g) into hexane fraction (HF), dichloromethane fraction (DF), ethyl acetate fraction (EF), methanol fraction (MF), and methanol insoluble residue (MR). Anti-collagenase activities were expressed as IC<sub>50</sub> (the half maximal inhibitory concentration) of MMP-1 and MMP-2, which are the matrix metalloproteinase type 1 and 2, respectively. All data are presented as mean  $\pm$  SD of triplicates.

### 3.6. Anti-Hair Loss Activities of *E. debile* Extracts via the Inhibition of 5 $\alpha$ -Reductase Enzyme

Figure 9 and Table 3 show the variation of 5 $\alpha$ -reductase inhibitory capacities of the *E. debile* extracts, depending on the extraction methods and solvents. The regression equation derived from the finasteride calibration curve was  $y = 187.84x - 4.3768$ ,  $R^2 = 0.9979$  and used to compute FEA values. Extracts with a higher FEA value have a stronger inhibitory activity. All extracts showed inhibitions against 5 $\alpha$ -reductase with the FEA values ranging from  $0.83 \pm 0.01$  to  $1.48 \pm 0.06$  mg finasteride/g extract, representing the inhibitions between  $44.59 \pm 0.40$  and  $83.07 \pm 3.46\%$ . Anti-5 $\alpha$ -reductase activities were ranked by FEA values and %inhibition as the following: DF, EF, HF, MF, MR, and CE. The DF displayed the strongest 5 $\alpha$ -reductase inhibition ( $83.07 \pm 3.46\%$ ). HF and EF showed comparative capacities of inhibitions at  $60.86 \pm 0.39$  and  $62.45 \pm 0.83\%$ , respectively. CE, MR, and MF exhibited similar inhibitions at  $44.59 \pm 0.40$ ,  $46.99 \pm 0.34$ , and  $48.60 \pm 3.27\%$ , respectively. This suggests that the solvent–solvent partitioning method was able to isolate 5 $\alpha$ -reductase inhibitors from CE, particularly by dichloromethane, which is the solvent with a moderate polarity index. The presence of previously reported fatty acids and phytosterols in *E. debile* might be responsible for 5 $\alpha$ -reductase inhibitory effects.

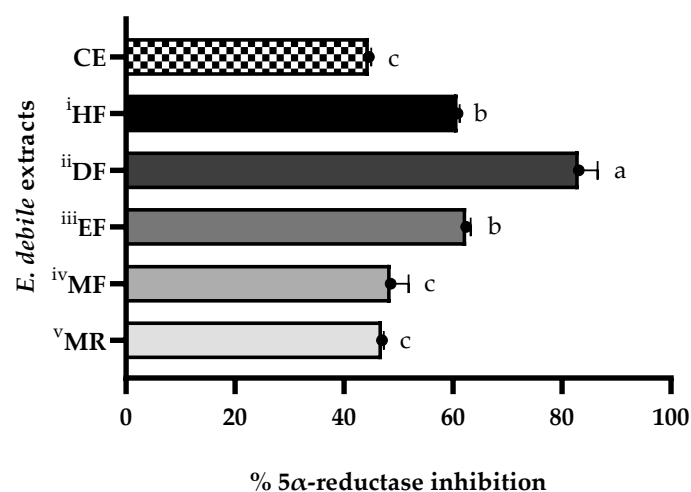


**Figure 9.** Anti-5 $\alpha$ -reductase activities of *E. debile* extracts. <sup>i–v</sup> Successive partition of crude extract (CE) ( $10.45 \pm 1.20$  g) into hexane fraction (HF), dichloromethane fraction (DF), ethyl acetate fraction (EF), methanol fraction (MF), and methanol insoluble residue (MR). All data are presented as mean  $\pm$  SD of triplicates. Letters (a, b, and c) indicate significant differences of means between the groups based on Tukey's HSD one-way ANOVA ( $p$ -value  $< 0.05$ ).

### 3.7. Evaluation of Anti-Tyrosinase, Anti-Collagenase, and Anti 5 $\alpha$ -Reductase Activities of *E. debile* Extracts during Storage

Storage conditions can affect phytochemical stability, leading to changes in the potency and efficiency of extract bioactivities. Therefore, in the present study, all *E. debile* extracts were kept under an accelerated storage condition at 40 °C for three months to assess the stability of bioactivities as shown in Figure 10. No statistically significant differences were observed in the activities of tyrosinase and collagenase (MMP-1 and MMP-2) inhibitions between month 0 and month 3 of all extracts ( $p$ -value > 0.05). However, slightly decreased activities of 5 $\alpha$ -reductase inhibition for CE, HF, EF, and MR were observed to be significantly different after 3 months ( $p$ -value < 0.05).

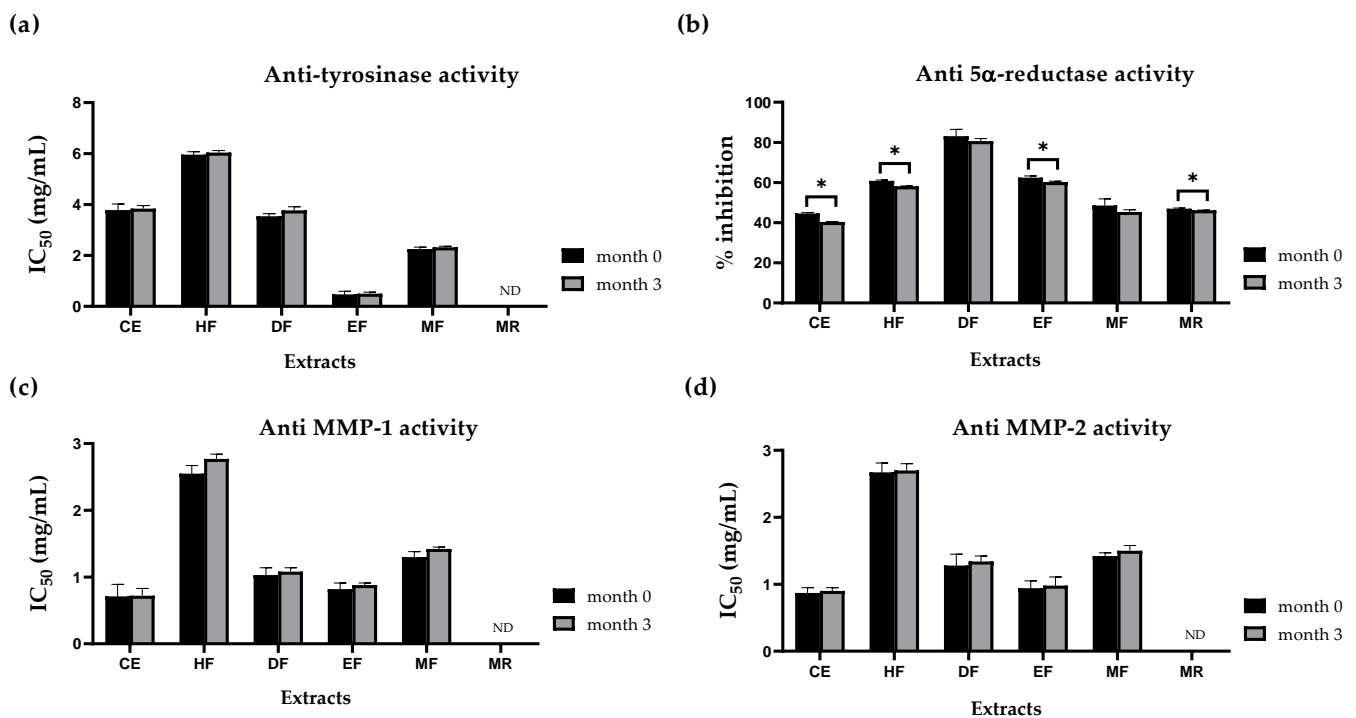


**Figure 10.** Stability potentials of the bioactivities of *E. debile* extracts during storage; (a) anti-tyrosinase activity; (b) anti-5 $\alpha$ -reductase activity; (c) anti-MMP-1 activity; and (d) anti-MMP-2 activity. Crude extract (CE) was successively partitioned to produce hexane fraction (HF), dichloromethane fraction (DF), ethyl acetate fraction (EF), methanol fraction (MF), and methanol insoluble residue (MR), respectively. All data are presented as mean  $\pm$  SD of triplicates. \* indicates statistically significant differences of means between month 0 and month 3 based on Student's  $t$ -test ( $p$ -value < 0.05).

### 3.8. In Vitro Cytotoxicity Test Using MTT Assay

The cytotoxicity of *E. debile* crude extracts and semi-purified fractions were evaluated in a skin fibroblast cell line (SF-TY) by the MTT assay. The highest cell viabilities were observed in the cell cultures treated with CE, EF, MF and MR, which also exhibited viabilities higher than 50% across all tested concentrations (Figure 11).

The lowest concentration tested at 1 mg/mL of CE, EF, MF and MR had cell viabilities higher than 80% after 24 h exposure, whereas HF and DF extracts had less than 80% cell viability. Cell viability decreased with increasing concentrations of all *E. debile* extracts. The IC<sub>50</sub> of *E. debile* extracts on the SF-TY cell line was also calculated to indicate the highest concentration of plant extracts that inhibits the cell viability at 50%. The MR had the highest IC<sub>50</sub> of  $14.62 \pm 0.25$  mg/mL, which was followed by CE ( $13.48 \pm 0.37$  mg/mL), EF ( $13.12 \pm 0.62$  mg/mL), MF ( $11.05 \pm 0.13$  mg/mL), DF ( $4.53 \pm 0.12$  mg/mL), and HF ( $4.22 \pm 0.61$  mg/mL). In general, lower IC<sub>50</sub> value represents higher toxicity.

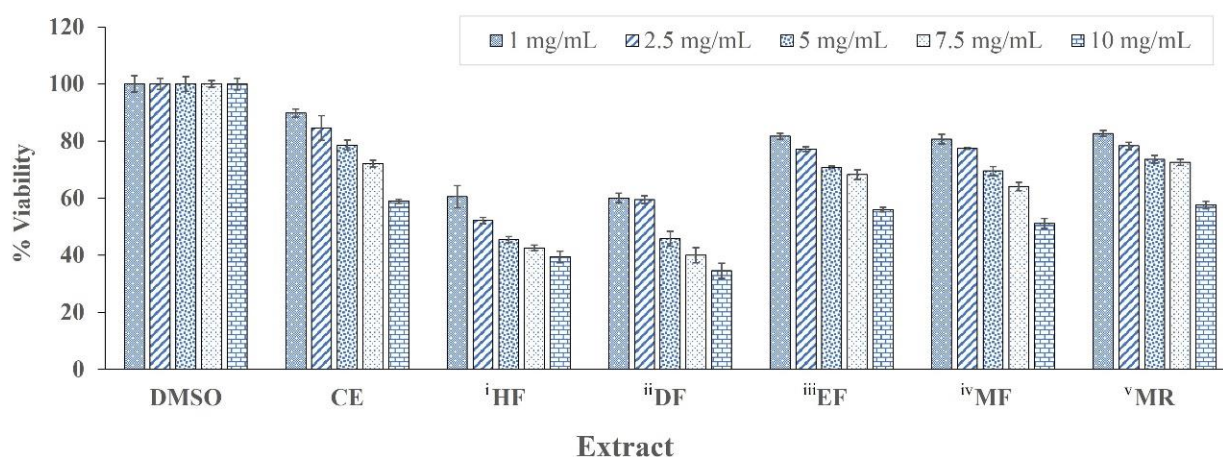


**Figure 11.** Cell viability study of *E. debile* extracts on skin fibroblast cell line (SF-TY) using MTT assay. <sup>i-v</sup> Successive partition of crude extract (CE) ( $10.45 \pm 1.20$  g) into hexane fraction (HF), dichloromethane fraction (DF), ethyl acetate fraction (EF), methanol fraction (MF), and methanol insoluble residue (MR). All data are presented as mean  $\pm$  SD of triplicates.

#### 4. Discussion

Phytochemicals have benefits to human health. However, their extractabilities are influenced by chemical structures. Therefore, extraction methods must be optimized to efficiently isolate compounds of interest. Macerations were previously used to obtain extracts from *E. debile*. Nonetheless, they may have limited usage due to the low content of bioactive compounds and less bioactivities as a result. Therefore, this study is the first report that aims to demonstrate the application of a solvent–solvent extraction technique to sequentially isolate phytochemicals by polar characteristics to obtain semi-purified fractions of *E. debile*. The macerated ethanolic crude extract of *E. debile* was successively partitioned by various solvents with increasing polarities as follows: hexane, dichloromethane, ethyl acetate, and methanol (Figures 1–3). Among these fractions, HF and DF had noticeably higher extractable yields than those of EF and MF (Figure 3). The highest extract yield was obtained by using hexane ( $43.64 \pm 1.80\%$ ). Additionally, the extract yield of HF was higher than that of DF by 1.82-fold. Based on the chemical polarities, each fraction should exhibit three main characteristics that are distinct from the crude extract. First, each fraction should reflect higher refined compound suites encompassing several chemicals with similar polarities than crude extract. Second, the quantities of particular compounds should be more concentrated in certain fractions than those of crude extract and other fractions. Third, individual fractions should represent a collection of phytochemicals that comprise the total composition of the crude extract. Therefore, this study may suggest that the majority of compounds in CE possessed the non-polar indices similarly to hexane, following by the compounds with moderate polarity indices similarly to dichloromethane. On the contrary, the extract yield of EF was the lowest among fractions and lower than that of MF by 2.72-fold. Taken together, the sequential partitioning method may enable the isolation of *E. debile* extracts with distinguishable phytochemicals. However, further experiments are required to identify the extracted compounds and examine the compound enrichments. The extraction yield is not only affected by solvent polarity but also other factors including growth conditions, time of harvesting, storage conditions, and extraction temperature. These factors should also be taken into consideration when designing and optimizing extraction methods.

*E. debile* extracts were further investigated for phenolic, silicon, and cosmeceutical potentials. The total phenolic contents (TPC) of *E. debile* extracts were shown in Figure 5. EF contained the highest TPC among fractions and was also higher than that of the crude extract by 2.19-fold. The TPC values obtained from DF and HF were comparative and the lowest among fractions. EF exhibited higher TPC than those of DF and HF by 8.98 and

11.1-fold, respectively. Additionally, MF displayed higher TPC than those of DF and HF by 2.22 and 2.75-fold. This indicates that most phenolic compounds in *E. debile* possessed moderate polarity characteristics in molecules predominantly close to and exclusively extractable by ethyl acetate. Two flavonoids, quercetin and quercetin-3-O- $\alpha$ -D-rhamnopyranoside, were previously isolated from the ethyl acetate extract of *E. debile* [55]. Therefore, these two compounds may be present in EF in this study. In addition, the phenolic compounds shown in Supplementary Table S1 were qualified from CE of *E. debile* by LCMS (Q-TOF) analysis. These compounds, including hypolaetin 8-rhamnoside, naringenin-7-O- $\beta$ -D-glucuronide, luteolin 7-glucoside, and kaempferol, may also be present in EF.

Silicon is known to strengthen skin, hair, nails, and bone [36,37]. In this study, silicon in *E. debile* extracts was determined by the ICP-OES method. The contents varied between 0.004 and 0.033% (Table 2), which was considerably low because *Equisetum* spp. are known to accumulate large amounts of silicon, around 5 to 10% as SiO<sub>2</sub> [26]. This could be partly explained by different sample types used in silicon analysis. In this study, silicon contents were investigated from the crude extract and its corresponding fractions rather than the whole plant. However, the results shown in this study were in accordance with the previous study of *E. sylvaticum* that reported only 0.025% of the total silicon was collectively extracted by a sequential extraction with solvents having different lipophilic properties [35]. This reaffirms that the extraction method in this study was not the optimal option to acquire high yield silicon. However, some minute silicon from *E. debile* extracts was detected. Among fractions, HF showed the highest silicon content, which was followed by DF, EF, MF, and MR. The results also show that MF yielded lower silicon content than that of HF by 1.83-fold. This could be partly explained by the potential formation of silicon complexes in plant cells. The accumulated silicon in some plants such as rice and cotton are known to form interactions and binding to organic matters in plant tissue [56]. The organic matrices in question might be made from polymers of carbohydrates such as cellulose, hemicellulose, and callose. These polymers are the major components of cell walls and possibly the sites of silicon deposition [57]. Interactions between organic compounds and silicon form complexes that alter silicon solubility. As a result, the silicon becomes less soluble in water and would only be liberated from plant tissue upon harsh treatment with strong acid digestion [35]. Taken together, this study may suggest that silicon might accumulate in *E. debile* tissue as the complex forms with a variety of solubilities, potentially with a preference of solubility to solvents with a lower range of polarity indices.

Melanin is a brown pigment causing skin to darken. Melanin biosynthesis depends on tyrosinase activations. The modulation of tyrosinase is regulated by not only an individual's genetics but also the responses to environmental stresses, particularly UV radiation [6,8,11]. Lowering melanin production has been proven to lighten dark skin. Therefore, the skin-whitening property of *E. debile* extracts was investigated via the inhibition of tyrosinase using a modified dopachrome 96-well plate method. The variation of inhibitory capacities among extracts was associated with solvent polarities and extraction methods (Figure 7 and Table 3). EF exerted the strongest tyrosinase inhibition. It was considerably stronger than that of HF by 114-fold KAE value and 13-fold IC<sub>50</sub> value. The findings in this study agreed with a previous study which reported the ethyl acetate extract from *E. ramosissimum* showing a protection against melanoma by decreasing melanin via several mechanisms, including inhibition of tyrosinase, oxidation, and expression of melanogenesis-related proteins, microphthalmia-associated transcription factor (MITF), and tyrosinase-related protein 1 and 2 (Trp-1 and Trp-2) [58]. Since *E. debile* and *E. ramosissimum* are in the same genus of *Equisetum*, the ethyl acetate extracts from these two horsetails may possess similar phytochemicals that exert similar mechanisms involving melanin. In this study, EF also possessed the highest total phenolic content among all extracts. Phenolics are known to inhibit tyrosinase and the oxidative process [59,60]. Therefore, the tyrosinase inhibitors in EF could be phenolic compounds. This explanation is also supported by a positive correlation between *E. debile* total phenolic content and the inhibition activity of tyrosinase

(coefficient of determination ( $R^2$ ) of 0.8587), as shown in Figure 6. Quercetin previously found in ethyl acetate extract of *E. debile* might be one of the bioactive phenolics that is responsible for the tyrosinase inhibitory effects [55]. Quercetin could inhibit tyrosinase via several mechanisms, such as the inhibition of monophenolase and diphenolase activities of tyrosinase [59,61]. It could directly bind to tyrosinase via hydrophobic interaction, leading to the induction of conformational changes and impeding enzymatic activities. Since the active site of tyrosinase contains binuclear copper, inhibitors could chelate the copper ion within active sites, leading to the obstruction of interaction between tyrosine substrate and tyrosinase. Quercetin bearing a catechol structure was previously known to chelate copper ion in tyrosinase active site [61]. Additionally, since hydroxylated flavonoids share structural similarities to tyrosine, it could also compete for tyrosinase [59,60]. In addition, the phenolic compounds found in CE by LCMS (Q-TOF) qualification analysis, such as hypolaetin 8-rhamnoside, naringenin-7-O- $\beta$ -D-glucuronide, luteolin 7-glucoside, and kaempferol, could also be compounds of interest due to their previously reported abilities to exert inhibitions against tyrosinase [62,63].

Collagens are proteins providing the structural stability of skin. Collagens account for 70–80% of skin weight and are known to be rapidly dismantled by collagenase. The depletion of collagens is a hallmark of wrinkle formation and aging skin [14]. The occurrence of diminishing collagens is strongly associated with UV-induced collagenases. Inhibitions of collagenases have been proved to delay collagen loss [64]. There is still a lack of anti MMP-1 and MMP-2 activity studies in the horsetail plants. This study therefore is the first to assess the inhibition of collagenase via MMP-1 and MMP-2 of *E. debile* extracts by using EnzChek assay kits. All *E. debile* extracts exhibited dose-dependent inhibitions against both collagenases, and the inhibition patterns between MMP-1 and MMP-2 were strongly consistent (Figure 8). CE and EF possessed comparative inhibitions and were the most potent against both enzymes. Among the fractions, EF had noticeably higher inhibitions than those of HF by 3.11-fold of  $IC_{50}$  MMP-1 and 2.84-fold of  $IC_{50}$  MMP-2. Although EF had similar inhibition potencies relative to CE, it is proposed as a superior extract for anti-wrinkle applications due to the higher refined compounds and richer phenolic contents. The EF's strong collagenase inhibitions could be partly explained by the enriched compositions of TPC. In polyphenol molecules, hydroxyl groups could directly interact with either backbone or other functional group side chains of collagenases. Additionally, the benzene ring of the molecule could form hydrophobic interactions to collagenases. These interactions lead to conformational changes, causing collagenase to be inactivated [64]. Another potential mechanism is that the phenolics directly chelate  $Zn^{2+}$  in the active site of collagenases since *Equisetum* plants were reported to have metal-chelating capacities for antioxidant activities [58]. The chelation prevents collagenases from interacting with collagen substrates. As a result, collagen degradation can be avoided, improving the condition of aging skin [47,60,65]. In this study, one of the phenolic compounds in *E. debile* extracts exerting these mechanisms could be quercetin, since it was previously shown to have the inhibitory effects against both the activities of recombinant human MMP-1 ( $IC_{50}$  of 39.6  $\mu$ M) and the induction of MMP-1 in human dermal fibroblasts via several mechanisms. These mechanisms include the inhibitions of extracellular signal-regulated protein kinase (ERK) and p38 mitogen-activated protein kinase (MAPK) [66]. Additionally, quercetin could down-regulate the expression of MMP-1 via an inhibition of activator protein-1. This study shows that the inhibition activities of MMP-1 and MMP-2 could be partially explained by total phenolic content with the coefficient of determination ( $R^2$ ) of 0.4127 and 0.5101, respectively (Figure 6). Moreover, phenolic compounds found in CE by LCMS (Q-TOF) qualification analysis, such as naringenin-7-O- $\beta$ -D-glucuronide, luteolin 7-glucoside, and kaempferol, could be the candidates for further study due to their previously reported involvements in the inhibitions against collagenases [67–69].

Collectively, this study demonstrates that *E. debile* extracts may be well suited for skin care and treatments. EF is the most attractive fraction for skin-whitening and anti-wrinkle applications. *E. debile* phenolics and flavonoids could be responsible for the inhibitions of

tyrosinase and collagenases. Although quercetins were previously identified in *E. debile* [55], further studies are still required to assess the total flavonoid content in the present study. The identification and quantification analysis of quercetins and other phenolic compounds shown in Supplementary Table S1 should also be investigated in the semi-purified fractions in order to infer their potential association with the observed inhibitory activities against tyrosinase and collagenases.

Dihydrotestosterone (DHT) is a potent androgen derivative. It is an essential hormone for normal male growth. However, highly expressed DHT is a major cause of androgenic alopecia [50]. The 5 $\alpha$ -reductase is a microsomal enzyme that is responsible for the reduction of testosterone to DHT. Therefore, the anti-hair loss activities of *E. debile* extracts were assessed via the inhibitions against 5 $\alpha$ -reductase (Figure 9 and Table 3). All extracts of *E. debile* exerted inhibitions against 5 $\alpha$ -reductase, ranging from 44.59  $\pm$  0.40 to 83.07  $\pm$  3.46%. DF displayed the strongest inhibition (FEA of 1.48  $\pm$  0.06 mg finasteride/g). CE and MF exhibited comparative inhibitions and were the lowest at 44.59  $\pm$  0.40 and 48.60  $\pm$  3.27%, respectively. HF and EF showed comparative inhibition potencies of 60.86  $\pm$  0.39 and 62.45  $\pm$  0.83%, respectively. The anti-5 $\alpha$ -reductase activity of *Equisetum* plants was previously reported from only *E. debile* species [32]. The findings in this present study agree with the previous investigation of *E. debile*, which reported the extracts from ethyl acetate, hexane, and ethanol exhibiting inhibitions against 5 $\alpha$ -reductase. However, this study is the first to report the inhibitory activities of semi-purified fractions of *E. debile* crude extracts against 5 $\alpha$ -reductase. Moreover, it is the first to express the activities of *E. debile* extract as an FEA value. In this study, dichloromethane rather than either hexane or ethyl acetate was able to sequester the strongest 5 $\alpha$ -reductase inhibitors, suggesting that phytochemicals conferring the most potent inhibitions preferred the solvents with the low range of moderate polarity indices. This study also shows that the total phenolic content was not related to the inhibition activity of 5 $\alpha$ -reductase (Figure 6). Fatty acids and phytosterols were speculated to be the compounds exerting anti-5 $\alpha$ -reductase activities due to their presences and potential mechanisms. Generally, hair growth treatments incorporate the active ingredients of lipophilic compounds containing several fatty acids including palmitic acid, stearic acid, oleic acid, linoleic acid, arachidic acid, and myristic acid. This is probably due to certain aliphatic free fatty acids exerting inhibitions against 5 $\alpha$ -reductase [70]. The structure of fatty acids, including chain length, unsaturation, oxidation, and esterification are factors that influenced the inhibition potencies. Fatty acids with C12–C16 chains and the presence of double bonds could enhance the inhibitions against 5 $\alpha$ -reductase.  $\beta$ -sitosterol isolated from the hexane fraction of *Dendropanax morbifera* showed the capacity to delay hair loss and improve hair density in mice [71]. However,  $\beta$ -sitosterol is less potent than finasteride in the inhibition of 5 $\alpha$ -reductase as demonstrating by the IC<sub>50</sub> of 2.7  $\mu$ M and 10.12 nM, respectively [72]. For *Equisetum* plants, the presence of fatty acids and phytosterols could therefore be responsible for the anti-5 $\alpha$ -reductase activity. Moreover, stigmasterol and daucosterol were previously isolated from *E. debile* [55]. Fatty acids and phytosterols are both lipophilic. Therefore, the usages of hexane, dichloromethane, and ethyl acetate may enable the sequestration of fatty acids and phytosterols into the fractions during the solvent–solvent partitioning of crude extract. Taken together, fatty acids and phytosterols may be responsible for HF, DF, and EF exhibiting stronger 5 $\alpha$ -reductase inhibition than CE and MF. Nonetheless, the direct associations between these compounds and the underline mechanisms need to be further characterized in *E. debile*. Some flavonoids, such as fisetin, genistein, and kaempferol, found in CE by LCMS (Q-TOF) qualification analysis in the present study, were previously reported to inhibit 5 $\alpha$ -reductase activity [73]. These flavonoids may be the responsible compounds in the EF.

Currently, finasteride is the only oral drug approved by the US FDA and the European Medicines Agency (EMA) to treat androgenic alopecia. A current recommended and marketed dosage of finasteride is 1 mg per day [2]. Although it is efficacious for hair regrowth, it causes severe side effects such as malignant neoplasms of male breast, sexual disorder, and high-grade prostate cancer. Thus, finasteride is often limited to only short-

term use. Therefore, exploring advantages of constituents from natural origins could lead to a discovery of novel compounds and functions. This study demonstrates such advantages from *E. debile*. The crude extract of *E. debile* had an FEA of 0.83 mg/mL, and all semi-purified fractions had FEA values ranging from 0.90 to 1.48 mg/mL. Therefore, a regular intake of *E. debile* extracts may be a possible natural alternative to chemically synthetic finasteride in preventing and treating androgenic alopecia.

Altogether, quercetin and fatty acids could be active compounds of *E. debile* for skin and hair benefits. Figure 10 shows that all extracts maintained inhibitory activities against tyrosinase and collagenase during a three-month storage period. On the other hand, only DF and MF maintained the anti-5 $\alpha$ -reductase activities, whereas CE, HF, EF, and MR activities were significantly decreased; however, they still had relevant values. Quercetin is a phenolic compound that can undergo many chemical changes by the oxidative process during food processing and storage. The oxygen concentration, pH, temperature, concentration of other antioxidants, as well as the presence of metal ions are known factors affecting the chemical stability of quercetin [74]. Additionally, the fatty acid composition of oils, especially the level of unsaturation, may influence the oxidative stability of the oil [75]. Therefore, further investigation of oxidative stabilities is suggested as the important quality control parameters of both phenolics and fatty acids in *E. debile* extracts for their potential cosmeceutical applications. This is the first study to report the stability of *E. debile* extracts by the determination of cosmeceutical potentials of anti-tyrosinase, anti-collagenases, and anti-5 $\alpha$ -reductase activities at three months storage under an accelerated condition at 40 °C. However, the bioactivity stability should be monitored beyond a three-month period.

In the present study, the cytotoxic effects of *E. debile* crude extract and semi-purified fractions at concentrations ranging from 1 to 10 mg/mL were investigated on a human skin fibroblast (SF-TY) cell line by using the MTT assay (Figure 11). Cell viabilities were evaluated after 24 h exposure to *E. debile* extracts. The CE, EF, MF and MR at 10 mg/mL showed cell viability higher than 50% and the IC<sub>50</sub> were above 10 mg/mL. The HF and DF (1 to 10 mg/mL) had cell viabilities ranging from approximately 35 to 60%. Previously, *E. debile* ethyl acetate extract showed no cytotoxicity on a dermal papilla cell line (1 to 1000  $\mu$ g/mL) and no irritation on the chorioallantoic membrane of hen's eggs (0.5% *w/v*) [32]. Further studies in other relevant cell lines and *in vivo* studies are required to ensure their safety.

## 5. Conclusions

This study explores the potential usage of *E. debile* extracts for cosmeceuticals applications by *in vitro* enzymatic assessments. The EF is suggested to contain the most attractive ingredients for hyperpigmentation, wrinkles, and skin aging treatments due to highly enriched total phenolic contents, exerting tyrosinase and collagenase inhibitions. The DF, HF, and EF are suggested as promising ingredients for hair loss treatment due to 5 $\alpha$ -reductase inhibitions. Additionally, compared to the recommended intake of finasteride (1 mg/day) for androgenic alopecia, the DF (1.48  $\pm$  0.06 mg finasteride/g) is proposed as an alternative source to naturally remediate hair loss.

Nonetheless, further studies are required to identify and investigate the active phytochemical compositions of *E. debile* crude extract and semi-purified fractions for better understanding of the mechanisms, pharmacodynamics, pharmacokinetics, side effects, and toxicities relating to their potential benefits as natural cosmeceutical alternatives. Cell-based assays are advised to confirm the observed *in vitro* inhibitory activities against tyrosinase, collagenases, and 5 $\alpha$ -reductase. The direct association between *E. debile* extracts and the cellular mechanisms could be further studied by investigating the changes in relevant gene expressions and the presences of melanin, collagen, and dihydrotestosterones. Most of the available safety information of *E. debile* extracts has been investigated using cell lines. The preliminary cytotoxicity shown in the present study may help provide useful information for further evaluation of *in vivo* and animal models, which would be essential for the cosmeceutical usage of *E. debile* in topical applications for skin and hair care. In

addition, the development of formulations providing the controlled release of plant extracts may help improve their skin biocompatibility [76].

**Supplementary Materials:** The following supporting information can be downloaded at: <https://www.mdpi.com/article/10.3390/app13031336/s1>, Table S1. Proposed phenolic compounds in *E. debile* by LCMS qualitative identification.

**Author Contributions:** Conceptualization, P.T., J.J. and S.S.; validation, P.T., J.J. and S.S.; formal analysis, P.T., J.J. and S.S.; investigation, P.T., J.J., K.S. and S.S.; resources, P.T., J.J., S.S., R.P., A.R. and H.P.; data curation, P.T., J.J. and S.S.; writing—original draft preparation, P.T.; writing—review and editing, P.T., J.J. and S.S.; visualization, P.T. and J.J.; supervision, P.T., J.J. and S.S.; project administration, S.S.; funding acquisition, P.T., J.J., S.S., R.P., A.R. and H.P. All authors have read and agreed to the published version of the manuscript.

**Funding:** This research was funded by the Highland Research and Development Institute (Public Organization, Chiang Mai, Thailand) (grant number 5/2560 and 17/2562) and partially supported from Fundamental Fund, Chiang Mai University and Thailand Science Research and Innovation, Thailand (Grant number FRB650031/0162\_FF65/047).

**Institutional Review Board Statement:** This article contains an assay using donated and unused rat livers obtained from the control group of an unrelated study performed by Khat-udomkiri et al., 2020 [51], in which the rats were euthanized, and all experiment protocols were approved by the Research Animal Care and Use Ethical Committee, Faculty of Pharmacy, Chiang Mai University, Thailand (Ethics approval no. 04/2015), in compliance with the National Institutes of Health and ARRIVE guidelines for the care and treatment of animals.

**Informed Consent Statement:** Not applicable.

**Data Availability Statement:** All the related data has been provided in the manuscript.

**Acknowledgments:** The article processing charge (APC) was supported by Center of Excellence for Innovation in Analytical Science and Technology for Biodiversity-Based Economic and Society (I-ANALY-S-T\_B.BES-CMU), Chiang Mai University, Chiang Mai, Thailand.

**Conflicts of Interest:** All authors declare no conflict of interest.

## References

1. Jiang, J.; Akinseye, O.; Tovar-Garza, A.; Pandya, A. The effect of melasma on self-esteem: A pilot study. *Int. J. Women's Dermatol.* **2018**, *4*, 38–42. [[CrossRef](#)] [[PubMed](#)]
2. Stough, D.; Stenn, K.; Haber, R.; Parsley, W.M.; Vogel, J.E.; Whiting, D.A.; Washenik, K. Psychological effect, pathophysiology, and management of androgenetic alopecia in men. *Mayo Clin. Proc.* **2005**, *80*, 1316–1322. [[CrossRef](#)] [[PubMed](#)]
3. Assaf, H.; Adly, M.; Hussein, M. Aging and Intrinsic Aging, Pathogenesis and Manifestations. In *Textbook of Aging Skin*; Farage, M.A., Miller, K.W., Maibach, H.I., Eds.; Springer: Berlin/Heidelberg, Germany, 2010; pp. 129–138.
4. Demeule, M.; Brossard, M.; Pagé, M.; Gingras, D.; Béliveau, R. Matrix metalloproteinase inhibition by green tea catechins. *Biochim. Biophys. Acta Prot. Struct. Mol. Enzym.* **2000**, *1478*, 51–60. [[CrossRef](#)] [[PubMed](#)]
5. Fisher, G.J.; Kang, S.; Varani, J.; Bata-Csorgo, Z.; Wan, Y.; Datta, S.; Voorhees, J.J. Mechanisms of photoaging and chronological skin aging. *Arch. Dermatol.* **2002**, *138*, 1462–1470. [[CrossRef](#)] [[PubMed](#)]
6. Schallreuter, K.U.; Kothari, S.; Chavan, B.; Spencer, J.D. Regulation of melanogenesis—controversies and new concepts. *Exp. Dermatol.* **2008**, *17*, 395–404. [[CrossRef](#)] [[PubMed](#)]
7. Sim, G.S.; Lee, B.C.; Cho, H.S.; Lee, J.W.; Kim, J.H.; Lee, D.H.; Kim, J.H.; Pyo, H.B.; Moon, D.C.; Oh, K.W.; et al. Structure activity relationship of antioxidative property of flavonoids and inhibitory effect on matrix metalloproteinase activity in UVA-irradiated human dermal fibroblast. *Arch. Pharm. Res.* **2007**, *30*, 290–298. [[CrossRef](#)]
8. Winder, A.; Kobayashi, T.; Tsukamoto, K.; Urabe, K.; Aroca, P.; Kameyama, K.; Hearing, V.J. The tyrosinase gene family—interactions of melanogenic proteins to regulate melanogenesis. *Cell Mol. Biol. Res.* **1994**, *40*, 613–626.
9. Brenner, M.; Hearing, V.J. The protective role of melanin against UV damage in human skin. *Photochem. Photobiol.* **2008**, *84*, 539–549. [[CrossRef](#)]
10. Nicolaidou, E.; Katsambas, A.D. Pigmentation disorders: Hyperpigmentation and hypopigmentation. *Clin. Dermatol.* **2014**, *32*, 66–72. [[CrossRef](#)]
11. Rigopoulos, D.; Gregoriou, S.; Katsambas, A. Hyperpigmentation and melasma. *J. Cosmet. Dermatol.* **2007**, *6*, 195–202. [[CrossRef](#)]
12. Brett, D.A. review of collagen and collagen-based wound dressings. *Wounds* **2008**, *20*, 347–356. [[PubMed](#)]
13. Vu, T.H.; Werb, Z. Matrix metalloproteinases: Effectors of development and normal physiology. *Genes Dev.* **2000**, *14*, 2123–2133. [[CrossRef](#)] [[PubMed](#)]

14. Takema, Y.; Hattori, M.; Aizawa, K. The relationship between quantitative changes in collagen and formation of wrinkles on hairless mouse skin after chronic UV irradiation. *J. Dermatol. Sci.* **1996**, *12*, 56–63. [[CrossRef](#)] [[PubMed](#)]
15. Hamilton, J. Male pattern hair loss in man: Types and incidence. *Ann. N. Y. Acad. Sci.* **1951**, *53*, 708–728. [[CrossRef](#)] [[PubMed](#)]
16. Severi, G.; Sinclair, R.; Hopper, J.L.; English, D.R.; McCredie, M.R.E.; Boyle, P.; Giles, G.G. Androgenetic alopecia in men aged 40–69 years: Prevalence and risk factors. *Br. J. Dermatol.* **2003**, *149*, 1207–1213. [[CrossRef](#)]
17. Kaufman, K.D. Androgens and alopecia. *Mol. Cell Endocrinol.* **2002**, *198*, 89–95. [[CrossRef](#)]
18. Demark-Wahnefried, W.; Halabi, S.; Paulson, D.F. Serum androgens: Associations with prostate cancer risk and hair patterning. *J. Androl.* **1997**, *18*, 495–500. [[CrossRef](#)]
19. Signorello, L.B.; Wu, J.; Hsieh, C.C.; Tzonou, A.; Trichopoulos, D.; Mantzoros, C.S. Hormones and hair patterning in men: A role for insulin-like growth factor 1? *J. Am. Acad. Dermatol.* **1999**, *40*, 200–203. [[CrossRef](#)]
20. Olumide, Y.M.; Akinkugbe, A.O.; Altraide, D.; Mohammed, T.; Ahamefule, N.; Ayanlowo, S.; Onyekonwu, C.; Essen, N. Complications of chronic use of skin lightening cosmetics. *Int. J. Dermatol.* **2008**, *47*, 344–353. [[CrossRef](#)]
21. Fischer, T.; Perosino, E.; Poli, F.; Viera, M.S.; Dreno, B. Chemical peels in aesthetic dermatology: An update 2009. *J. Eur. Acad. Dermatol. Venereol.* **2010**, *24*, 281–292. [[CrossRef](#)]
22. Rendon, M.I.; Berson, D.S.; Cohen, J.L.; Roberts, W.E.; Starker, I.; Wang, B. Evidence and considerations in the application of chemical peels in skin disorders and aesthetic resurfacing. *J. Clin. Aesthet. Dermatol.* **2010**, *3*, 32–43. [[PubMed](#)]
23. Carneiro, D.M.; Jardim, T.V.; Araújo, Y.C.L.; Arantes, A.C.; Sousa, A.C.; Barroso, W.K.S.; Sousa, A.L.L.; Cunha, L.C.; Cirilo, H.N.C.; Bara, M.T.F.; et al. *Equisetum arvense*: New evidences supports medical use in daily clinic. *Pharmacogn. Rev.* **2019**, *13*, 50–58. [[CrossRef](#)]
24. Schaffner, J.H. Geographic distribution of the species of *Equisetum* in relation to their phylogeny. *Am. Fern. J.* **1930**, *20*, 89–106. [[CrossRef](#)]
25. Badole, S.; Kotwal, S. *Equisetum arvense*: Ethanopharmacological and Phytochemical review with reference to osteoporosis. *Int. J. Pharm. Sci. Health Care* **2014**, *1*, 131–141.
26. Law, C.; Exley, C. New insight into silica deposition in horsetail (*Equisetum arvense*). *BMC Plant Biol.* **2011**, *11*, 112. [[CrossRef](#)]
27. Pekmezci, E.; Dündar, C.; Türkoğlu, M. A proprietary herbal extract against hair loss in androgenetic alopecia and telogen effluvium: A placebo-controlled, single-blind, clinical-instrumental study. *Acta Derm. Alp Pannon Adriat* **2018**, *27*, 51–57. [[CrossRef](#)]
28. Alexandru, V.; Gaspar, A.; Savin, S.; Toma, A.; Tatia, R.; Gille, E. Phenolic content, antioxidant activity and effect on collagen synthesis of a traditional wound healing polyherbal formula. *Stud. Univ. Vasile Goldis Arad Ser. Stiint. Vietii* **2015**, *25*, 41–46.
29. Al-Snafi, A.E. The pharmacology of *Equisetum arvense*-A review. *IOSR J. Pharm.* **2017**, *7*, 31–42. [[CrossRef](#)]
30. Carneiro, D.M.; Freire, R.C.; Deus Honório, T.C.; Zoghaib, I.; Cardoso, F.F.S.E.S.; Tresvenzol, L.M.F.; Paula, J.R.; Sousa, A.L.L.; Jardim, P.C.B.V.; Cunha, L.C. Randomized, double-blind clinical trial to assess the acute diuretic effect of *Equisetum arvense* (field horsetail) in healthy volunteers. *Evid. Based Complement Altern. Med.* **2014**, *2014*, 760683. [[CrossRef](#)]
31. Council of Europe. *European Pharmacopoeia*, 8th ed.; European Directorate for the Quality of Medicines & Healthcare, Council of Europe: Strasbourg, France, 2015; pp. 2013–2014.
32. Chaiyana, W.; Punyoyai, C.; Somwongin, S.; Leelapornpisid, P.; Ingkaninan, K.; Waranuch, N.; Srivilai, J.; Thitipramote, N.; Wisuitiprot, W.; Schuster, R.; et al. Inhibition of 5 $\alpha$ -reductase, IL-6 secretion, and oxidation process of *Equisetum debile* Roxb. ex vaucher extract as functional food and nutraceuticals ingredients. *Nutrients* **2017**, *9*, 1105. [[CrossRef](#)]
33. Kanchanapoom, T.; Otsuka, H.; Ruchirawat, S. Megastigmane glucosides from *Equisetum debile* and *E. diffusum*. *Chem. Pharm. Bull.* **2007**, *55*, 1277–1280. [[CrossRef](#)] [[PubMed](#)]
34. Sarkar, B.; Raihan, S.M.A.; Sultana, N.; Rahman, R.; Islam, M.E.; Ahmed, S.; Akter, S. Cytotoxic, antibacterial and free radical scavenging activity studies of the solvent extracts of aerial stems of *Equisetum debile* Roxb. *Int. J. Chem. Sci.* **2012**, *10*, 19–26.
35. Bye, R.; Thingstad, S.F.; Paulsen, B.S. Horsetail (*Equisetum* spp.) as a Source of Silicon Supplement in Human Nutrition—A Myth? *J. Herbs Spices Med. Plants* **2010**, *16*, 119–125. [[CrossRef](#)]
36. Wickett, R.R.; Kossmann, E.; Barel, A.; Demeester, N.; Clarys, P.; Vanden Berghe, D.; Calomme, M. Effect of oral intake of choline-stabilized orthosilicic acid on hair tensile strength and morphology in women with fine hair. *Arch. Dermatol. Res.* **2007**, *299*, 499–505. [[CrossRef](#)]
37. Barel, A.; Calomme, M.; Timchenko, A.; De Paepe, K.; Demeester, N.; Rogiers, V.; Clarys, P.; Vanden Berghe, D. Effect of oral intake of choline-stabilized orthosilicic acid on skin, nails and hair in women with photodamaged skin. *Arch. Dermatol. Res.* **2005**, *297*, 147–153. [[CrossRef](#)] [[PubMed](#)]
38. Organización Mundial de la Salud and World Health Organization. *WHO Guidelines on Good Agricultural and Collection Practices (GACP) for Medicinal Plants*; World Health Organization: Geneva, Switzerland, 2003.
39. European Medicines Agency. *Guideline on Good Agricultural and Collection Practice (GACP) for Starting Materials of Herbal Origin*; European Medicines Agency Evaluation of Medicines for Human Use: London, UK, 2006; pp. 1–11.
40. Chatha, S.A.S.; Anwar, F.; Manzoor, M. Evaluation of the antioxidant activity of rice bran extracts using different antioxidant assays. *Grasas Y Aceites* **2006**, *57*, 328–335.
41. Siddhuraju, P.; Becker, K. Antioxidant properties of various solvent extracts of total phenolic constituents from three different agroclimatic origins of drumstick tree (*Moringa oleifera* Lam.) leaves. *J. Agric Food Chem.* **2003**, *51*, 2144–2155. [[CrossRef](#)] [[PubMed](#)]

42. Sultana, B.; Anwar, F.; Ashraf, M. Effect of extraction solvent/technique on the antioxidant activity of selected medicinal plant extracts. *Molecules* **2009**, *14*, 2167–2180. [[CrossRef](#)]
43. Emran, T.B.; Rahman, A.; Uddin, M.N.; Rahman, M.; Uddin, Z.; Dash, R.; Layzu, C. Effects of organic extracts and their different fractions of five Bangladeshi plants on *in vitro* thrombolysis. *BMC Complement Altern Med.* **2015**, *15*, 128. [[CrossRef](#)]
44. Thammarat, P.; Sirilun, S.; Phongpradist, R.; Raiwa, A.; Pandith, H.; Jiaranaikulwanitch, J. Validated HPTLC and antioxidant activities for quality control of catechin in a fermented tea (*Camellia sinensis* var. *assamica*). *Food Sci. Nutr.* **2021**, *9*, 3228–3239. [[CrossRef](#)]
45. Fox, C. Advances in cosmetic science and technology. IV: Skin care and treatment. *Cosmet. Toilet.* **1995**, *110*, 63–93.
46. Chattuwatthana, T.; Okello, E. Anti-collagenase, anti-elastase and antioxidant activities of *Pueraria candollei* var. *mirifica* root extract and *Coccinia grandis* fruit juice extract: An *in vitro* study. *Eur. J. Med. Plants* **2015**, *5*, 318–327. [[CrossRef](#)]
47. Bigg, H.F.; Clark, I.M.; Cawston, T.E. Fragments of human fibroblast collagenase: Interaction with metalloproteinase inhibitors and substrates. *Biochim. Biophys. Acta Prot. Struct. Mol. Enzym.* **1994**, *1208*, 157–165. [[CrossRef](#)]
48. Eun Lee, K.; Bharadwaj, S.; Yadava, U.; Gu Kang, S. Evaluation of caffeine as inhibitor against collagenase, elastase and tyrosinase using *in silico* and *in vitro* approach. *J. Enzym. Inhib. Med. Chem.* **2019**, *34*, 927–936. [[CrossRef](#)]
49. EnzChek™ Gelatinase/Collagenase Assay Kit. Available online: <https://assets.fishersci.com/TFS-Assets/LSG/manuals/mp12052.pdf> (accessed on 5 January 2023).
50. Kumar, T.; Chaiyasut, C.; Rungseevijitprapa, W.; Suttajit, M. Screening of steroid 5 $\alpha$ -reductase inhibitory activity and total phenolic content of Thai plants. *J. Med. Plant Res.* **2011**, *5*, 1265–1271.
51. Khat-udomkiri, N.; Toejing, P.; Sirilun, S.; Chaiyasut, C.; Lailerd, N. Antihyperglycemic effect of rice husk derived xylooligosaccharides in high-fat diet and low-dose streptozotocin-induced type 2 diabetic rat model. *Food Sci. Nutr.* **2020**, *8*, 428–444. [[CrossRef](#)] [[PubMed](#)]
52. Lowry, O.; Rosebrough, N.; Farr, A.; Randall, R. Protein determination by a modified Folin phenol method. *J. Biol. Chem.* **1951**, *193*, 265–275. [[CrossRef](#)] [[PubMed](#)]
53. Oliveira, J.R.; Castro, V.C.; Graças Figueiredo Vilela, P.; Camargo, S.E.A.; Carvalho, C.A.T.; Jorge, A.O.C.; Oliveira, L.D. Cytotoxicity of Brazilian plant extracts against oral microorganisms of interest to dentistry. *BMC Complement Altern Med.* **2013**, *13*, 208. [[CrossRef](#)] [[PubMed](#)]
54. Hazekawa, M.; Nishinakagawa, T.; Kawakubo-Yasukochi, T.; Nakashima, M. Evaluation of IC<sub>50</sub> levels immediately after treatment with anticancer reagents using a real time cell monitoring device. *Exp. Ther. Med.* **2019**, *18*, 3197–3205. [[CrossRef](#)]
55. Sarkar, B.; Raihan, S.; Sultana, N.; Islam, M.E. Isolation of two steroids and two flavonoids having antioxidant, antibacterial and cytotoxic properties from aerial stems of *Equisetum debile* Roxb. *Nat. Univ. J. Sci.* **2014**, *1*, 31–42.
56. Inanaga, S.; Okasaka, A.; Tanaka, S. Does silicon exist in association with organic compounds in rice plant? *Soil. Sci. Plant Nutr.* **1995**, *41*, 111–117. [[CrossRef](#)]
57. Perry, C.C.; Lu, Y. Preparation of silicas from silicon complexes: Role of cellulose in polymerisation and aggregation control. *J. Chem. Soc. Faraday Trans.* **1992**, *88*, 2915–2921. [[CrossRef](#)]
58. Li, P.H.; Chiu, Y.P.; Shih, C.C.; Wen, Z.H.; Ibetto, L.K.; Huang, S.H.; Chiu, C.C.; Ma, D.L.; Leung, C.H.; Chang, Y.N.; et al. Biofunctional activities of *Equisetum ramosissimum* extract: Protective effects against oxidation, melanoma, and melanogenesis. *Oxid. Med. Cell Longev.* **2016**, *2016*, 2853543. [[CrossRef](#)] [[PubMed](#)]
59. Jeong, S.H.; Ryu, Y.B.; Curtis-Long, M.J.; Ryu, H.W.; Baek, Y.S.; Kang, J.E.; Lee, W.S.; Park, K.H. Tyrosinase inhibitory polyphenols from roots of *Morus lhoui*. *J. Agric. Food Chem.* **2009**, *57*, 1195–1203. [[CrossRef](#)]
60. Malešev, D.; Kuntić, V. Investigation of metal-flavonoid chelates and the determination of flavonoids via metal-flavonoid complexing reactions. *J. Serb Chem. Soc.* **2007**, *72*, 921–939. [[CrossRef](#)]
61. Fan, M.; Zhang, G.; Hu, X.; Xu, X.; Gong, D. Quercetin as a tyrosinase inhibitor: Inhibitory activity, conformational change and mechanism. *Food Res. Int.* **2017**, *100*, 226–233. [[CrossRef](#)]
62. El-Nashar, H.A.; El-Din, M.I.G.; Hritcu, L.; Eldahshan, O.A. Insights on the inhibitory power of flavonoids on tyrosinase activity: A survey from 2016 to 2021. *Molecules* **2011**, *26*, 7546. [[CrossRef](#)]
63. Rho, H.S.; Ghimeray, A.K.; Yoo, D.S.; Ahn, S.M.; Kwon, S.S.; Lee, K.H.; Cho, D.H.; Cho, J.U. Kaempferol and kaempferol rhamnosides with depigmenting and anti-inflammatory properties. *Molecules* **2011**, *16*, 3338–3344. [[CrossRef](#)]
64. Madhan, B.; Krishnamoorthy, G.; Rao, J.R.; Nair, B.U. Role of green tea polyphenols in the inhibition of collagenolytic activity by collagenase. *Int. J. Biol. Macromol.* **2007**, *41*, 16–22. [[CrossRef](#)]
65. McDonald, M.; Mila, I.; Scalbert, A. Precipitation of metal ions by plant polyphenols: Optimal conditions and origin of precipitation. *J. Agric Food Chem.* **1996**, *44*, 599–606. [[CrossRef](#)]
66. Lim, H.; Kim, H.P. Inhibition of mammalian collagenase, matrix metalloproteinase-1, by naturally-occurring flavonoids. *Planta Med.* **2007**, *73*, 1267–1274. [[CrossRef](#)]
67. Balli, U.; Cetinkaya, B.O.; Keles, G.C.; Keles, Z.P.; Guler, S.; Sogut, M.U.; Erisgin, Z. Assessment of MMP-1, MMP-8 and TIMP-2 in experimental periodontitis treated with kaempferol. *J. Periodontal. Implant. Sci.* **2016**, *46*, 84–95. [[CrossRef](#)] [[PubMed](#)]
68. Hwang, Y.P.; Oh, K.N.; Yun, H.J.; Jeong, H.G. The flavonoids apigenin and luteolin suppress ultraviolet A-induced matrix metalloproteinase-1 expression via MAPKs and AP-1-dependent signaling in HaCaT cells. *J. Dermatol. Sci.* **2011**, *61*, 23–31. [[CrossRef](#)] [[PubMed](#)]

69. Jung, S.K.; Ha, S.J.; Jung, C.H.; Kim, Y.T.; Lee, H.K.; Kim, M.O.; Lee, M.H.; Mottamal, M.; Bode, A.M.; Lee, K.W.; et al. Naringenin targets ERK 2 and suppresses UVB-induced photoaging. *J. Cell Mol. Med.* **2016**, *20*, 909–919. [[CrossRef](#)] [[PubMed](#)]
70. Liu, J.; Shimizu, K.; Kondo, R. Anti-androgenic activity of fatty acids. *Chem. Biodivers* **2009**, *6*, 503–512. [[CrossRef](#)]
71. Lee, S.Y.; Choi, E.J.; Bae, D.H.; Lee, D.W.; Kim, S. Effects of 1-tetradecanol and  $\beta$ -sitosterol isolated from *Dendropanax morbifera* Lev. on skin whitening, moisturizing and preventing hair loss. *J. Soc. Cosmet. Sci. Korea* **2015**, *41*, 73–83. [[CrossRef](#)]
72. Cabeza, M.; Eugene, B.; Ivonne, H.; Elena, R.L.; Mauricio, S.; Eugenio, F. Effect of  $\beta$ -sitosterol as Inhibitor of  $5\alpha$ -reductase in Hamster Prostate. *Proc. West Pharm. Soc.* **2003**, *46*, 153–155.
73. Hiipakka, R.A.; Zhang, H.Z.; Dai, W.; Dai, Q.; Liao, S. Structure–activity relationships for inhibition of human  $5\alpha$ -reductases by polyphenols. *Biochem. Pharm.* **2002**, *63*, 1165–1176. [[CrossRef](#)] [[PubMed](#)]
74. Wang, W.; Sun, C.; Mao, L.; Ma, P.; Liu, F.; Yang, J.; Gao, Y. The biological activities, chemical stability, metabolism and delivery systems of quercetin: A review. *Trends Food Sci. Technol.* **2016**, *56*, 21–38. [[CrossRef](#)]
75. Parker, T.D.; Adams, D.A.; Zhou, K.; Harris, M.; Yu, L. Fatty acid composition and oxidative stability of cold-pressed edible seed oils. *J. Food Sci.* **2003**, *68*, 1240–1243. [[CrossRef](#)]
76. Makhija, P.; Kathuria, H.; Sethi, G.; Grobber, B. Polymeric hydrogels for controlled release of black tea and coffee extracts for topical applications. *Gels* **2021**, *7*, 174. [[CrossRef](#)] [[PubMed](#)]

**Disclaimer/Publisher’s Note:** The statements, opinions and data contained in all publications are solely those of the individual author(s) and contributor(s) and not of MDPI and/or the editor(s). MDPI and/or the editor(s) disclaim responsibility for any injury to people or property resulting from any ideas, methods, instructions or products referred to in the content.